Table 2. Incidence of carcinoma and quantitative evaluation of neoplastic lesions in ventral and lateral prostate

Treatment	Number of rats	Ventral				Lateral			
		Incidence of carcinoma	% of lesions in prostate			Incidence of carcinoma	% of lesions in prostate		
			LG-PIN	HG-PIN	Carcinoma		LG-PIN	HG-PIN	Carcinoma
Control	11	11 (100%)	6.6 ± 2.5	81.8 ± 4.8	11.7 ± 4.5	10 (91%)	11.8 ± 5.2	82.8 ± 6.8	5.4 ± 3.9
100 mg/L	11	11 (100%)	8.0 ± 2.5	83.6 ± 3.8	8.4 ± 2.8*	10 (91%)	17.4 ± 4.3	80.1 ± 4.3	2.5 ± 1.4*
500 mg/L	11	11 (100%)	8.3 ± 1.6	87.3 ± 3.2**	4.4 ± 1.9***	6 (55%)	26.8 ± 9.9***	71.8 ± 9.0**	1.5 ± 1.7**

*,**,***Indicate significant difference from the control group, $P < 0.05$, 0.1, 0.001, respectively.

Table 3. Labeling indices of Ki67 and 8-OHdG in HG-PIN of ventral and lateral prostate

Treatment	Ventral prostate		Lateral prostate	
	Ki67	8-OHdG	Ki67	8-OHdG
Control	52.6 ± 1.1	2.9 ± 0.4	49.7 ± 1.6	2.7 ± 0.4
100 mg/L	43.8 ± 2.2***	2.3 ± 0.4**	35.2 ± 7.2***	2.0 ± 0.2***
500 mg/L	24.4 ± 1.8***	1.5 ± 0.3***	18.4 ± 2.8***	1.5 ± 0.2***

**, ***Significantly different from control group, $P < 0.01$, 0.001, respectively.

1.7 ± 1.0 and 1.9 ± 0.8 ng/mL, respectively) but that of estradiol was not affected (control, 100 and 500 mg/L apocynin: 3.2 ± 1.0, 3.4 ± 1.2 and 3.3 ± 0.7 pg/mL, respectively). Adiponection concentration in the serum did not differ among the groups (control, 100 and 500 mg/L apocynin: 3.5 ± 1.1, 3.2 ± 0.5 and 3.5 ± 0.8 ng/mL, respectively).

Representative histopathological findings of ventral and lateral prostate in each group are presented in Figure 1(a). In the ventral prostate, there was a marked or partial pathologic response to apocynin treatment, as demonstrated by a significant reduction in the prostatic neoplastic lesions in TRAP rats; however, small foci of PIN remained. Decrease in the incidence of adenocarcinoma was also observed in the lateral prostate (Table 2). Quantitative evaluation of the proportion of preneoplastic and neoplastic lesions in the prostate gland showed significant suppression of progression from LG-PIN or HG-PIN to adenocarcinoma in rats treated with apocynin in a dose-dependent manner (Table 2). To focus on adenocarcinoma, the number of foci per area in both the ventral and lateral prostate was significantly reduced by apocynin in a dose-dependent manner (Fig. 1b,c). There was no difference in the average size of adenocarcinomas in both the ventral and lateral prostate among the groups (data not shown). There was a significant decrease in the labeling index of Ki-67 and 8-OHdG in HG-PIN of the ventral and lateral prostates of TRAP rats given apocynin in a dose-dependent manner (Table 3). Although the rate of significance was slightly less, the results were mostly the same in the adenocarcinoma of the ventral and lateral prostates (Table S1). Results for ROS detection in ventral prostate by dihydroethidium are presented in Figure 1(d), with significant reduction (11 and 22% reduction

Table 4. Upregulated and downregulated genes by apocynin treatment in ventral prostate

ID	Reference ID	Symbol	Description	Ratio
Upregulated genes				
ENSRNOG00000038093	–	LAC2_RAT	Ig lambda-2 chain C region	5.62
ENSRNOG00000033745	–	Q5FVP9_RAT	Cfh protein	3.10
ENSRNOG00000005743	NM_001108582.1	NP_001102052.1	LOC362136 (predicted) (RGD1309610_predicted), mRNA	2.58
ENSRNOG00000033615	–	NU3M_RAT	NADH-ubiquinone oxidoreductase chain 3 (EC 1.6.5.3)	2.45
ENSRNOG00000015155	NM_001037351.1	Tnnc2	Troponin C2, fast	2.11
ENSRNOG00000008746	NM_001108594.1	NP_001102064.1	Histidyl tRNA synthetase 2	2.07
ENSRNOG00000001333	NM_012826.1	Azgp1	Zinc-alpha-2-glycoprotein precursor	2.06
ENSRNOG00000002871	NM_001108984.1	NP_001102454.1	RNA binding motif protein 25	2.05
ENSRNOG00000023151	NM_203333.2	Scgb2a2	Secretoglobin family 2A member 2 precursor	2.01
Downregulated genes				
ENSRNOG00000021604	NM_001008835.1	RT1-CE1	RT1 class I, CE1	0.28
ENSRNOG00000002343	NM_017237.2	Uchl1	Ubiquitin carboxyl-terminal hydrolase isozyme L1 (EC 3.4.19.12)	0.36
ENSRNOG00000038999	NM_001008827.1	RT1-A1	RT1 class Ia, locus A1	0.36
ENSRNOG00000029579	NM_001008840.1	RT1-CE2	RT1 class I, CE2	0.41
ENSRNOG00000030251	–	RT1-CE10	RT1 class I, CE10	0.41
ENSRNOG00000032872	–	UBIQ_RAT	Ubiquitin	0.43
ENSRNOG00000034234	–	COX1_RAT	Cytochrome c oxidase subunit 1 (EC 1.9.3.1)	0.43
ENSRNOG00000037414	–	Q5I1B4_RAT	ABP beta (Fragment)	0.44
ENSRNOG00000030371	–	COX2_RAT	Cytochrome c oxidase subunit 2	0.45
ENSRNOG00000039668	NM_001107100.1	NP_001100570.1	Procollagen, type VIII, alpha 1	0.46
ENSRNOG00000016460	NM_053021.2	Clu	Clusterin precursor	0.49
ENSRNOG00000011647	NM_053485.2	S100a6	Protein S100-A6	0.50
ENSRNOG00000007539	NM_138881.1	Best5	Radical S-adenosyl methionine domain-containing protein 2	0.50
ENSRNOG00000002052	NM_022543.2	Ssg1	Coiled-coil domain-containing protein 80 precursor	0.50

doi: 10.1111/cas.12292

at 100 and 500 mg/L, respectively) documented (Fig. 1e). Androgen receptors and SV40 T antigen were diffusely detected immunohistochemically in areas of PIN and adenocarcinomas in the ventral and lateral prostate, with no differences among the groups (data not shown).

Reduction of cell proliferation by apocynin treatment was associated with changes in clusterin and the MEK-ERK1/2 pathway. To elucidate the mechanisms of anti-carcinogenesis of apocynin, microarray analysis was performed (GEO: GSE47200). Genes that were upregulated or downregulated by apocynin are listed in Table 4. After selection, 9 upregulated and 14 downregulated genes were detected, some related to oxidative responses (NADH-ubiquinone oxidoreductase chain 3, cytochrome c oxidase subunit 1 and 2) and others immunological responses (Ig lambda-2 chain C region, Cfh protein, secretoglobin family 2A member 2 precursor, RT1 class I, CE1, CE2 and CE10, RT1 class Ia, locus A1). Because apocynin reduced rat prostate carcinogenesis, we focused on the clusterin precursor belonging to downregulated genes, which is known to be related to tumorigenesis in many sites. Reduction of clusterin expression in the ventral prostate of apocynin-treated rats was confirmed by real-time RT-PCR (Fig. 1f) and also by western blotting (Fig. 1g). Immunohistochemical analyses revealed that clusterin expression was observed mainly in the epithelial membranes of the ventral prostate of TRAP rats, but no staining was observed in the epithelium of the prostate of Sprague–Dawley rats (Fig. S1a). Differences in the intensity of clusterin immunostaining determined by optical density measurement was relatively inconspicuous among LG-PIN, HG-PIN or adenocarcinoma in the ventral lobes of the control TRAP rats (Fig. S1b). However, clusterin expression in HG-PIN of ventral prostate of apocynin-treated TRAP rats was significantly reduced compared to the control (Fig. S1c; control, 100 and 500 mg/L apocynin: 50.1 ± 5.0, 43.2 ± 7.4 and 35.6 ± 4.3, respectively). Reduction of phosphorylation in MEK and p44/42 MAPK (ERK1/2), and cyclin D1 were also detected. Cleaved caspases 3 and 7 were detected in the ventral prostate of some apocynin-treated rats (Fig. 1h).

Apocynin affected reduction of cell growth via the same pathways in a human prostate cancer cell line. In the human prostate cell line, significant reduction of cell growth and ROS generation was detected after apocynin treatment at concentrations higher than 250 μM (Fig. 2a,b). Apocynin-treated cells appeared to accumulate in G1 phase at 500 μM, compared to the controls ($P < 0.05$), with concomitant decrease in the percentage of cells in the S phase (Fig. 2c). Downregulation of clusterin around 70 kDa and cyclin D1 expression were detected by western blotting (Fig. 2d).

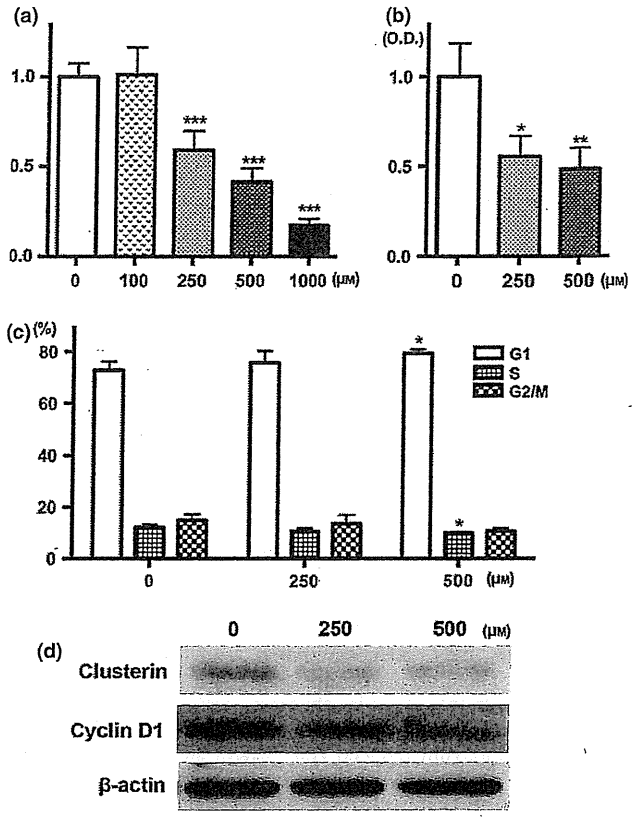

Fig. 2. Anti-growth effects of apocynin in LNCaP cells. Cells were incubated with apocynin for 72 h and then cytotoxicity was assessed by WST-1 assay (a). Reactive oxygen species production data detected by DCFH-DA after apocynin treatment for 24 h (b). Cell cycle distribution of LNCaP cells after treatment with apocynin for 24 h (c). Immunoblot analysis of the protein levels of clusterin, cyclin D1 and ß-actin with apocynin treatment (d). $*P < 0.05$, $**P < 0.01$ and $***P < 0.001$ compared to controls. O.D, optical density.

Discussion

In the present study, we demonstrated suppressive effects of apocynin treatment on prostatic carcinogenesis in the TRAP rat model. Because apocynin is known to be an NADPH oxidase inhibitor, we focused on ROS conditions in prostate tissue using immunohistochemistry for 8-OHdG and dihydroethidium staining. Some reports have indicated that antioxidants such as N-acetylcysteine and vitamin C clearly reduce oxidative stress *in vitro*, but exert less effects with oral dosing *in vivo*.[15,16] ROS is generally produced from mitochondria, peroxisomes, cytochrome P450 and NADPH oxidase.[4,6,7] Apocynin only affects ROS reduction from NADPH oxidase, but it would be expected to be a good antioxidant *in vivo*. In addition, we did not detect any toxic effects of apocynin in this study.

Reactive oxygen species generation is not only considered associated with tissue injury and/or DNA damage, but also neoplastic transformation, aberrant growth and/or proliferation.[4,7] Indeed, ROS may play broad roles in cellular processes associated with initiation and development of many cancers, including prostate cancer.[6] In this study, apocynin reduced the Ki-67 labeling index and cyclin D1 expression, which indicates that ROS generation is related to cell proliferation in prostate lobes of TRAP rats. Furthermore, NADPH oxidase is reported to regulate plasma adiponectin,[17] whose concentration may be negatively correlated with prostate cancer progression.[18] Therefore, we investigated adiponectin concentration in serum, but did not find any differences among the groups.

In TRAP rats, we previously detected activation of p38 MAPK and ERK1/2 in prostate tissue, and inactivation by chemopreventive agents such as angiotensin II receptor blocker or purple corn color.[14,19] These also reduced cell proliferation and/or induced apoptosis in prostate tissue. In this study, we also detected dephosphorylation of ERK1/2 in the prostate after apocynin treatment. To assess the relationship between ROS generation and phosphorylation of ERK1/2, microarray analysis was employed. The data obtained for upregulated and downregulated genes indicated associations with ROS generation, immune function and translation by gene ontology.[20] We focused on clusterin, dysregulated in many types of cancer, including prostate cancer,[21] with cellular functions such as a sulfated glycoprotein in regulation of apoptosis, cell cycle control, DNA repair, cell adhesion and tissue remodeling.[22,23] It has two isoforms. Secretory clusterin (sCLU) has a chaperone

action like that of small heat shock proteins, and is sized around 70–80 kDa. The other clusterin isoform is the nuclear form (nCLU) of 55 kDa, associated with cell death.[21–23] In this study, we detected significant reduction of clusterin protein around 70 kDa. Because sCLU is reported to be downregulated by p53 in some tumor cells,[22] high expression of clusterin in the prostate would be expected given dysfunction of p53 under the influence of SV40 T antigen in TRAP rats.[24]

In human prostate cancer, clusterin expression is initially low in contrast with the prostate cancer cells resistant to conventional chemotherapy or hormonal therapy which show upregulation.[21,25] Meanwhile, we detected rather high expression of clusterin in all stages of prostate cancer development in TRAP rats. In te transgenic adenocarcinoma of mouse prostate (TRAMP) model, higher expression of clusterin in the prostate glands was detected compared to that in non-transgenic mice; however, analyses of overt carcinoma revealed no expression.[26] These data suggest that SV40 T antigen supports to induce clusterin expression among the carcinogenic process in the prostate of both mice and rats. The difference in clusterin expression in carcinoma may be related to the different histology between mice (poorly-differentiated neuroendocrine-like carcinomas) and rats (moderately differentiated adenocarcinomas), because clusterin is mainly stained in the membrane.

Recently, sCLU was reported to induce phosphorylation of ERK1/2 in lung adenocarcinoma and pancreatic cancer cells.[27,28] Therefore, we considered that apocynin reduced prostate carcinogenesis via clusterin, acting on the ERK1/2 pathway and reducing cell proliferation in TRAP rats. We also found that apocynin reduced cell growth and ROS generation, along with expression of clusterin and cyclin D1 in LNCaP cells (human prostate cell line). Although there is a possibility that the exact intracellular molecular pathways affected by apocynin treatment may be different between humans and rats, we suggest that there may be similar anti-neoplastic effects caused by apocynin, especially related to clusterin expression, in rat and human prostate.

Chemoprevention attempts are comprehensive in prostate cancer, and various agents are reported to prevent, reverse or delay tumor deveolpment and progression.[29] In this study, we detected lower incidence of adenocarcinoma in the lateral lobes of 500 mg/L apocynin-treated rats, and reduction of cell proliferation was observed in both PIN and adenocarcinoma. Thus, we consider that apocynin has potential to prevent and delay the carcinogenic process, and is suitable as a chemopreventive drug. Recently, custirsen (OGX-011), a clusterin inhibitor, was selected for use as an anti-cancer drug in a randomized phase II study of patients with metastatic castration-resistant prostate cancer.[30,31] We earlier reported that apocynin inhibited growth of androgen-independent prostate cancer with inhibition of phosphorylation of Rac1 and NF-κB and angiogenesis.[32] Together with the present data, we confirm that apocynin has the potential to be a candidate anti-cancer drug for androgen-dependent/independent prostate cancer.

In conclusion, apocynin, an NADPH oxidase inhibitor, suppressed prostate carcinogenesis while reducing ROS in the TRAP rat model. The mechanism of prevention appears to involve regulation of cell proliferation via clusterin and the MEK-ERK1/2 pathway. Apocynin warrants further attention as a promising chemopreventive drug for prostate cancer.

Acknowledgments

This work was supported by a Grant-in-Aid for the 3rd Term Comprehensive 10-Year Strategy for Cancer Control from the Ministry of Health, Labour and Welfare of Japan and grants from Ono Pharmaceutical, the Society for Promotion of Pathology in Nagoya, and the Research Foundation for Oriental Medicine. The authors would like to thank Dr Malcolm Moore for his help in reviewing this manuscript.

Disclosure Statement

The authors have no conflict of interest.

References

1 Jemal A, Bray F, Center MM, Ferlay J, Ward E, Forman D. Global cancer statistics. *CA Cancer J Clin* 2011; **61**: 69–90.
2 Damber JE, Aus G. Prostate cancer. *Lancet* 2008; **371**: 1710–21.
3 Lee YJ, Lee JH, Han HJ. Extracellular adenosine triphosphate protects oxidative stress-induced increase of p21(WAF1/Cip1) and p27(Kip1) expression in primary cultured renal proximal tubule cells: role of PI3K and Akt signaling. *J Cell Physiol* 2006; **209**: 802–10.
4 Wu WS. The signaling mechanism of ROS in tumor progression. *Cancer Metastasis Rev* 2006; **25**: 695–705.
5 Kumar B, Koul S, Khandrika L, Meacham RB, Koul HK. Oxidative stress is inherent in prostate cancer cells and is required for aggressive phenotype. *Cancer Res* 2008; **68**: 1777–85.
6 Khandrika L, Kumar B, Koul S, Maroni P, Koul HK. Oxidative stress in prostate cancer. *Cancer Lett* 2009; **282**: 125–36.
7 Bedard K, Krause KH. The NOX family of ROS-generating NADPH oxidases: physiology and pathophysiology. *Physiol Rev* 2007; **87**: 245–313.
8 Stolk J, Hiltermann TJ, Dijkman JH, Verhoeven AJ. Characteristics of the inhibition of NADPH oxidase activation in neutrophils by apocynin, a methoxy-substituted catechol. *Am J Respir Cell Mol Biol* 1994; **11**: 95–102.
9 Stefanska J, Pawliczak R. Apocynin: molecular aptitudes. *Mediators Inflamm* 2008; **2008**: 106507.
10 Suzuki S, Arnold LL, Pennington KL, Kakiuchi-Kiyota S, Cohen SM. Effects of co-administration of dietary sodium arsenite and an NADPH oxidase inhibitor on the rat bladder epithelium. *Toxicology* 2009; **261**: 41–6.
11 Asamoto M, Hokaiwado N, Cho YM *et al.* Prostate carcinomas developing in transgenic rats with SV40 T antigen expression under probasin promoter control are strictly androgen dependent. *Cancer Res* 2001; **61**: 4693–700.
12 Cho YM, Takahashi S, Asamoto M *et al.* Age-dependent histopathological findings in the prostate of probasin/SV40 T antigen transgenic rats: lack of influence of carcinogen or testosterone treatment. *Cancer Sci* 2003; **94**: 153–7.
13 Seeni A, Takahashi S, Takeshita K *et al.* Suppression of prostate cancer growth by resveratrol in the transgenic rat for adenocarcinoma of prostate (TRAP) model. *Asian Pac J Cancer Prev* 2008; **9**: 7–14.
14 Long N, Suzuki S, Sato S *et al.* Purple corn color inhibition of prostate carcinogenesis by targeting cell growth pathways. *Cancer Sci* 2013; **104**: 298–303.
15 Wang Z, Zhou J, Lu X, Gong Z, Le XC. Arsenic speciation in urine from acute promyelocytic leukemia patients undergoing arsenic trioxide treatment. *Chem Res Toxicol* 2004; **17**: 95–103.
16 Gibson KR, Neilson IL, Barrett F *et al.* Evaluation of the antioxidant properties of N-acetylcysteine in human platelets: prerequisite for bioconversion to glutathione for antioxidant and antiplatelet activity. *J Cardiovasc Pharmacol* 2009; **54**: 319–26.
17 Furukawa S, Fujita T, Shimabukuro M *et al.* Increased oxidative stress in obesity and its impact on metabolic syndrome. *J Clin Invest* 2004; **114**: 1752–61.
18 Goktas S, Yilmaz MI, Caglar K, Sonmez A, Kilic S, Bedir S. Prostate cancer and adiponectin. *Urology* 2005; **65**: 1168–72.
19 Takahashi S, Uemura H, Seeni A *et al.* Therapeutic targeting of angiotensin II receptor type 1 to regulate androgen receptor in prostate cancer. *Prostate* 2012; **72**: 1559–72.
20 Ashburner M, Ball CA, Blake JA *et al.* Gene ontology: tool for the unification of biology. The Gene Ontology Consortium. *Nat Genet* 2000; **25**: 25–9.
21 Rizzi F, Bettuzzi S. The clusterin paradigm in prostate and breast carcinogenesis. *Endocr Relat Cancer* 2010; **17**: R1–17.
22 Shannan B, Seifert M, Leskov K *et al.* Challenge and promise: roles for clusterin in pathogenesis, progression and therapy of cancer. *Cell Death Differ* 2006; **13**: 12–9.
23 Shannan B, Seifert M, Boothman DA, Tilgen W, Reichrath J. Clusterin and DNA repair: a new function in cancer for a key player in apoptosis and cell cycle control. *J Mol Histol* 2006; **37**: 183–8.

doi: 10.1111/cas.12292

24 Ahuja D, Saenz-Robles MT, Pipas JM. SV40 large T antigen targets multiple cellular pathways to elicit cellular transformation. *Oncogene* 2005; **24**: 7729–45.
25 Rizzi F, Bettuzzi S. Clusterin (CLU) and prostate cancer. *Adv Cancer Res* 2009; **105**: 1–19.
26 Caporali A, Davalli P, Astancolle S *et al.* The chemopreventive action of catechins in the TRAMP mouse model of prostate carcinogenesis is accompanied by clusterin over-expression. *Carcinogenesis* 2004; **25**: 2217–24.
27 Chou TY, Chen WC, Lee AC, Hung SM, Shih NY, Chen MY. Clusterin silencing in human lung adenocarcinoma cells induces a mesenchymal-to-epithelial transition through modulating the ERK/Slug pathway. *Cell Signal* 2009; **21**: 704–11.
28 Tang Y, Liu F, Zheng C, Sun S, Jiang Y. Knockdown of clusterin sensitizes pancreatic cancer cells to gemcitabine chemotherapy by ERK1/2 inactivation. *J Exp Clin Cancer Res* 2012; **31**: 73.
29 Gupta S. Prostate cancer chemoprevention: current status and future prospects. *Toxicol Appl Pharmacol* 2007; **224**: 369–76.
30 Saad F, Hotte S, North S *et al.* Randomized phase II trial of Custirsen (OGX-011) in combination with docetaxel or mitoxantrone as second-line therapy in patients with metastatic castrate-resistant prostate cancer progressing after first-line docetaxel: CUOG trial P-06c. *Clin Cancer Res* 2011; **17**: 5765–73.
31 Chi KN, Hotte SJ, Yu EY *et al.* Randomized phase II study of docetaxel and prednisone with or without OGX-011 in patients with metastatic castration-resistant prostate cancer. *J Clin Oncol* 2010; **28**: 4247–54.
32 Suzuki S, Pitchakarn P, Sato S, Shirai T, Takahashi S. Apocynin, an NADPH oxidase inhibitor, suppresses progression of prostate cancer via Rac1 dephosphorylation. *Exp Toxicol Pathol* 2013; **65**: 1035–41.

Supporting Information

Additional supporting information may be found in the online version of this article:

Fig. S1. Expression of clusterin in ventral lobe of prostate. Pictures of H&E and immunohistochemistry of clusterin in normal epithelium in Sprague–Dawley rat, LG-PIN, HG-PIN and carcinoma in TRAP rats (a) and expression of clusterin (b). Expression of clusterin in HG-PIN of ventral lobe of control, 100 and 500 mg/L apocynin treated rats (c). Carcinoma; Adenocarcinoma. *,***$P < 0.05$ and 0.001 compared to Normal epithelium or control, respectively.

Table S1. Labeling indices of Ki67 and 8-OHdG in adenocarcinoma of ventral and lateral prostate.

*J Toxicol Pathol 2014; 27: **–****

Original Article

Establishment of an Invasive Prostate Cancer Model in Transgenic Rats by Intermittent Testosterone Administration

Shinya Sato[1], Shugo Suzuki[1], Aya Naiki-Ito[1], Masami Komiya[1, #], Long Ne[1, ##], Hiroyuki Kato[1], Hiroyuki Sagawa[1], Yoriko Yamashita[1], Tomoyuki Shirai[1, ###], and Satoru Takahashi[1]

[1] Department of Experimental Pathology and Tumor Biology, Nagoya City University Graduate School of Medical Sciences, 1 Kawasumi, Mizuho-cho, Mizuho-ku, Nagoya 467-8601, Japan

Abstract: We have established a transgenic rat for adenocarcinoma of the prostate (TRAP) model that features uniform adenocarcinoma development in prostatic lobes at high incidence within a short experimental period. However, no invasive carcinomas with reactive stroma characteristics similar to those in man were observed. We therefore have focused on a new model for invasive carcinoma of the prostate using TRAP rats. In experiment 1, male TRAP rats in groups 1 and 2 were treated with orchiectomy at day 0 of the experiment. Rats in groups 1–3 underwent testosterone propionate (TP) implantation from weeks 1 to 4 and from weeks 6 to 16. Rats in groups 1 and 3 were given 3,2'-dimethyl-4-aminobiphenyl (DMAB) after TP implantation. The rats of group 4 served as controls. In experiment 2, the rats were divided into three groups, none of which received DMAB or orchiectomy, treated with TP continuously or with the treatment withdrawn once or twice. In experiment 1, invasive adenocarcinomas with abundant collagenous stroma were found in the dorsolateral and anterior prostate, some of which showed perineural space invasion at week 16. The number of invasive carcinoma foci was most frequent in group 3. In experiment 2, invasive adenocarcinoma development in the lateral prostates was correlated with the number of TP administration/withdrawal cycles. In conclusion, our newly established rat model for invasive adenocarcinoma of the prostate could serve as a useful preclinical model for evaluating the *in vivo* efficacy of preventive and therapeutic agents targeting of the tumor microenvironment. (DOI: 10.1293/tox.27.**; J Toxicol Pathol 2014; 27: **–**)

Key words: prostate cancer, animal model, cancer invasion, transgenic rat, testosterone propionate, intermittent administration

Introduction

Prostate cancer is the most common cancer and the second leading cause of death from cancer among men in the US. It has been estimated there will be approximately 238,590 new cases of prostate cancer and 29,720 deaths from prostate cancer in the US in 2013[1]. In Japan, the prevalence and mortality of prostate cancer has also been increasing, along with in the so-called nutrition transition[2, 3]. Androgen ablation therapy is generally applied for prostate cancer because of hormone-dependent growth. However, outgrowth of androgen-independent and metastatic cancer cells is a frequent outcome, eventually leading to death of the patient. Therefore, understanding of the mechanisms of the acquisition of metastatic potential or the androgen-independent phenotype of cancer cells is urgently required.

We have established a rat cancer model responding to the need for *in vivo* systems that adequately reproduce the spectrum of human prostate cancers. Administration of 3,2'-dimethyl-4-aminobiphenyl (DMAB) induces noninvasive and androgen-dependent adenocarcinomas in the ventral prostate, while additional long-term treatment with testosterone propionate (TP) causes development of invasive and metastasizing androgen-independent adenocarcinomas arising from the dorsolateral and anterior prostate and seminal vesicles[4, 5]. However, a long period of about 60 weeks is required to induce prostate cancers in both carcinogenesis models, and the incidence of lesion development is relatively low. Therefore, we have established transgenic rats bearing a probasin promoter/simian virus 40 (SV40) T antigen construct to resolve these problems[6]. This model, the transgenic rat for adenocarcinoma of the prostate (TRAP), features development of high-grade prostatic intraepithelial neoplasia (HGPIN) from 4 weeks of age and androgen-dependent well-moderately differentiated adenocarcinomas with 100% incidences by the age of 15 weeks. These characteristics of the TRAP model have been shown to be

Received: 8 September 2013, Accepted: 28 October 2013
*Corresponding author: S Takahashi (e-mail: sattak@med.nagoya-cu.ac.jp)
Present: # Division of Cancer Prevention Research, National Cancer Center Research Institute, ****complete address****, Tokyo, Japan
Present: ## National Center for Geriatrics and Gerontology, ****complete address****, Obu, Japan
Present: ### Nagoya City Rehabilitation Center, ****complete address****, Nagoya, Japan

complete address が必要ですのでお知らせください。

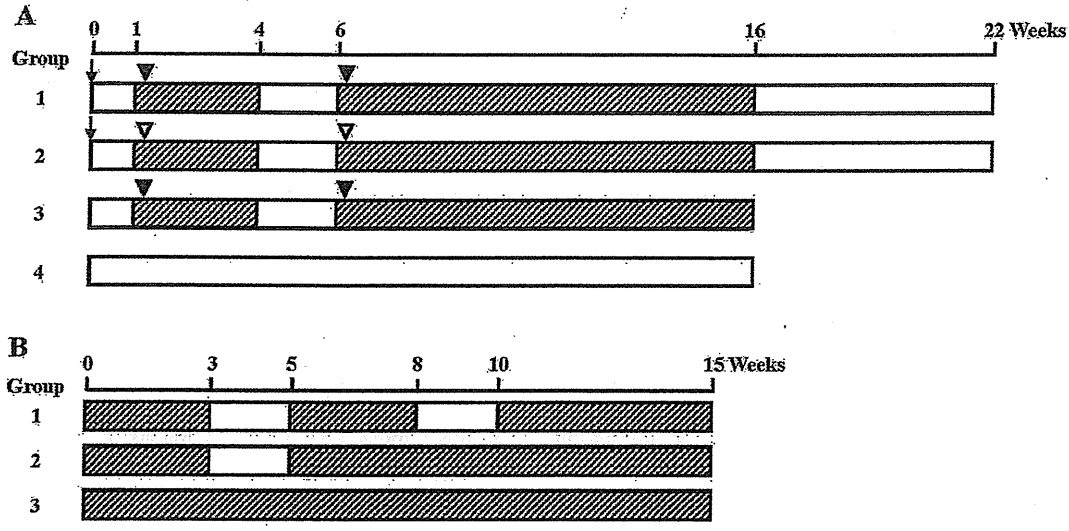

Fig. 1. Experimental design for experiments 1 (A) and 2 (B) for induction of invasive prostate adenocarcinomas in TRAP rats. The animals used were male TRAP rats that were 6 weeks of age at commencement of the study. Shaded, testosterone propionate, silicone rubber tube (40 mg); arrow, bilateral orchiectomy; filled arrowhead, DMAB 50 mg/kg b.w.; open arrowhead, vehicle (corn oil).

very suitable for evaluation of strategies for chemoprevention and treatment[7–10]. Microinvasive carcinomas characterized by a budding morphology from acini are observed in an age-dependent manner in TRAP rats, but these lesions are generally only 0.2–0.3 mm diameter in size and take over 35 weeks to develop[11]. We speculated that testosterone administration might be of paramount importance in the induction of invasive carcinoma in our transgenic rats based on our experience with the DMAB combined with TP-induced prostate carcinogenesis model. In the present study, we therefore assessed whether testosterone exposure might result in a high-grade invasive phenotype or metastatic lesions in TRAP rats.

Materials and Methods

Chemicals

TP was purchased from Sigma-Aldrich (St. Louis, MO, USA) and DMAB was obtained from Matsugaki Pharmaceutical Co. (Osaka, Japan). The purity of DMAB was >98%. Antibody for androgen receptor (AR) was obtained from Santa Cruz Biotechnology Inc (N-20, Santa Cruz, CA, USA). The antibody for Ki-67 was from Acris Antibodies GmbH (SP-6, Hiddenhausen, Germany).

Animals

Male heterozygous TRAP rats with a Sprague–Dawley genetic background were obtained from Oriental BioService Inc. (Minamiyamashiro, Kyoto, Japan) and were housed in plastic cages with hardwood chips in an air-conditioned room with a 12 h light/dark cycle at 23 ± 2°C and 50 ± 10% humidity. Food (Oriental MF; Oriental Yeast Co., Ltd., Tokyo, Japan) and tap water were available *ad libitum*. They were acclimatized for 1 week before use. Surgical treatments, such as orchiectomy and tube implantation, were carried out under deep isoflurane anesthesia. All animal experiments were performed under protocols approved by the Institutional Animal Care and Use Committee of the Nagoya City University Graduate School of Medical Sciences.

Experimental protocols

Experiment 1: A total of 24 male TRAP rats aged 6 weeks were randomly divided into four groups. Rats in groups 1 and 2 were treated with bilateral orchiectomy at day 0 of the experiment. Those in groups 1–3 underwent subcutaneous implantation of 2-cm-long silicone rubber tubes (Silascon®, inner diameter, 0.2 cm; outer diameter, 0.3 cm, Kaneka Medix Corporation, Osaka, Japan) containing 40 mg TP sealed at both ends with silicone rubber sealing compound (KE-42, Shin-Etsu Chemical Co., Ltd., Tokyo, Japan) into the interscapular region from weeks 1 to 4 and from weeks 6 to 16. The TP implants were replaced at 6-week intervals. Rats in groups 1 and 3 were subcutaneously given DMAB at a dose of 50 mg/kg body weight on the second day after TP tube implantation. No treatment was performed in rats of group 4, which served as controls. Animals were euthanized at weeks 16 and 22 after the beginning of the experiment (Fig.1A).

Experiment 2: A total of 24 heterozygous male TRAP rats aged 6 weeks were randomly divided into three groups. All were given TP implants in the same manner as in experiment 1 at day 0. The duration of TP administration was different among the groups; that is, TP was administered in experimental weeks 0–3, 5–8 and 10–15 in group 1 and

in experimental weeks 0–3 and 5–15 in group 2. Group 3 was continuously administered TP by implants throughout the experiment. The experiment was terminated at week 15 (Fig. 1B).

In both experiments, blood samples were collected from the abdominal aorta under deep anesthesia, and prostates were removed and fixed in formalin. For tissue preparation of prostate glands, four sagittal slices of the ventral prostate, two sagittal samples of the dorsolateral prostate including the urethra, and two transverse slices from each side of the anterior prostate including seminal vesicles were embedded in paraffin. Tissues were processed routinely and stained with hematoxylin and eosin for histopathological examination. Testosterone and estradiol levels in serum were analyzed using radioimmunoassays by a commercial laboratory (SRL, Inc., Tokyo, Japan).

Immunohistochemistry

Deparaffinized sections were incubated with diluted antibodies for AR and Ki-67. The immunohistochemical analysis was performed with a Discovery XT System (Ventana Medical Systems, Tucson, AZ, USA). Incubation with primary antibodies was carried out for 3 hours followed by a one hour incubation with biotinylated anti-rabbit secondary antibody (Vectastain ABC Kit Rabbit IgG, Vector Laboratories, Burlingame, CA, USA) and a DAB detection kit (Ventana Medical Systems) according to the manufacturer's instructions. Sections were counterstained with hematoxylin to facilitate orientation.

Immunofluorescence

Deparaffinized sections were autoclaved at 120°C for 20 min in antigen retrieval solution (Nichirei Biosciences Inc.) and then allowed to cool. Sections were incubated with 1% skim milk for 1 hour at room temperature. For double staining, anti-smooth muscle actin antibodies (1A4, dilution 1:1,000, mouse monoclonal, Dako) and anti-vimentin antibodies (EPR3776, dilution 1:400, rabbit monoclonal, Abcam) were simultaneously added to the slides and incubated for 1 hour at room temperature. After washing the slides with PBS, fluorescein-labeled goat anti mouse IgG (Life Technologies Corporation.) and tetramethylrhodamine-labeled goat anti-rabbit IgG (Life Technologies Corporation.) were added followed by incubation at room temperature for 1 hour. After washing the slides with PBS, the sections were mounted with Vectashield containing DAPI (Vector Laboratories) and subjected to fluorescence microscopy.

Results

Experiment 1

At week 16, foci of invasive adenocarcinoma with abundant collagenous stroma were found in lateral, dorsal and anterior prostates of groups 1–3 (Fig. 2A, B, D, E), along with minute ventral invasive carcinomas with minimal fibrous stroma. Cancer invasion into perineural spaces was also observed (Fig. 2E). Almost all of infiltrating carcinoma cells expressed AR (Fig. 2C, F). The incidences of invasive adenocarcinoma varied among the groups, tending to be higher in group 3 in all prostatic lobes (Table 1). Similarly, the number of invasive carcinoma foci was highest in group 3 (Table 1). There were no differences in histopathological characteristics of invasive adenocarcinomas among the groups. Development of small cell carcinomas of the prostate was sporadically noted, but there were no differences in incidence among the groups. No metastasis of cancer lesions to distant organs was found in any of the groups. Noninvasive adenocarcinomas in the ventral, lateral prostates were observed in all rats of groups 1–4.

At week 22, neoplastic lesions of the prostates were completely resolved with massive involution in all rats of groups 1 and 2. This indicated that all of the invasive adenocarcinomas developed in prostate glands were androgen-dependent (data not shown).

Experiment 2

The results of experiment 1 indicated that bilateral orchiectomy or DMAB administration did not deeply contribute to efficient induction of invasive adenocarcinomas. Thus, we focused on whether TP administration/withdrawal was important.

A significant increase of invasive adenocarcinoma development was observed in group 1, and this correlated well with the number of TP administration/withdrawal cycles in the lateral prostates (Table 2). Multicentric development of invasive adenocarcinoma foci with abundant collagenous stroma was found (Fig. 3A–D), and invasive cancer cells were observed in the stroma (Fig. 3E) and were positive for AR protein (Fig. 3F). Some invasive lesions consisted of cells with atrophic features, but more than 50% of these cells were labeled for Ki-67, suggesting that they were high-grade adenocarcinomas (Fig. 3G). Reactive stromal cells surrounding invasive cancers expressed both smooth muscle actin and vimentin and were therefore revealed to be cancer-associated myofibroblasts (Fig. 4). Noninvasive adenocarcinomas in the ventral and lateral prostates were found in all rats of groups 1–3.

Discussion

The TRAP rat features sequential progression from prostatic intraepithelial neoplasias (PINs) to noninvasive adenocarcinomas through prostate epithelial cell-specific expression of the SV40 T antigen regulated by the androgen-dependent probasin promoter. We have applied the TRAP rat model to validate the chemopreventive effects of a variety of chemicals, and cancer development in TRAP rats is very sensitive to chemicals that modulate the AR axis, such as flutamide, finasteride, resveratrol or angiotensin II receptor blockers [7, 9, 12]. These characteristics underly its acceptability to mimic early-stage hormone naïve human prostate cancer without an invasive phenotype.

In the present study, we established a novel rat model for invasive adenocarcinoma of the prostate in TRAP rats

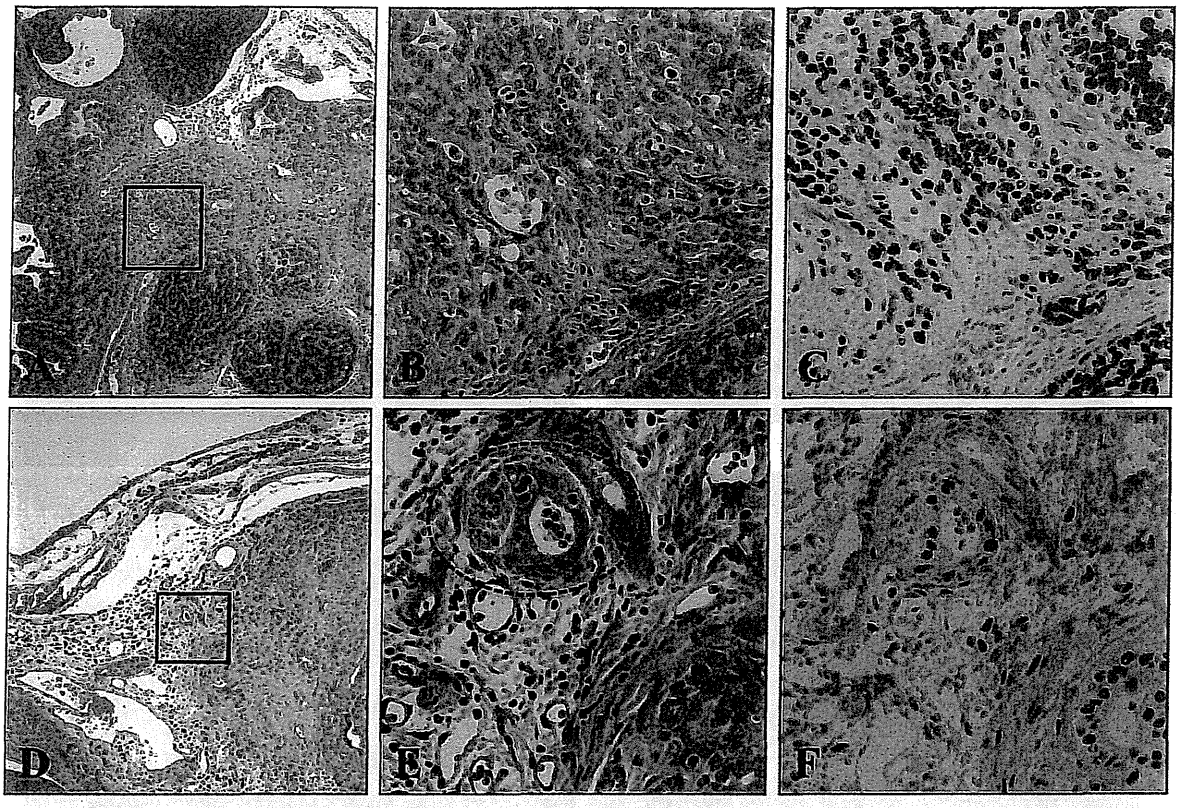

Fig. 2. Representative histopathological findings of invasive adenocarcinomas of the lateral prostate in group 3 (A–C) and anterior prostate in group 2 (D–F). Low (A, D) and high (B, E) magnifications of lateral and anterior prostates at week 16 after after the beginning of experiment 1. The rectangles in (A) and (D) represent the areas from (B) and (E), respectively. The dotted circle in (E) indicates perineural cancer invasion. (C, F) AR immunohistochemistry.

Table 1. Incidence and Multiplicity of Invasive Adenocarcinoma (at Week 16, Experiment 1)

Group	No. of rats	Lateral		Ventral		Dorsal		Anterior	
		Incidence (%)	No. of foci	Incidence (%)	No. of foci	Incidence (%)	No. of foci	Incidence (%)	No. of foci
1	5	1 (20)	0.20 ± 0.45	4 (80)	1.80 ± 1.64	1 (20)	0.20 ± 0.45	3 (60)	0.80 ± 0.84
2	4	2 (50)	1.00 ± 1.15	3 (75)	3.75 ± 3.78	1 (25)	0.25 ± 0.50	3 (75)	2.75 ± 3.10
3	4	4 (100)	4.00 ± 1.41[a,b]	4 (100)	6.00 ± 2.45[c]	3 (75)	1.00 ± 0.82	4 (100)	2.00 ± 0.82
4	5	2 (40)	0.40 ± 0.55	1 (20)	0.20 ± 0.45	0	-	2 (40)	0.40 ± 0.55

[a] $P<0.001$ vs groups 1 and 4; [b] $P<0.01$ vs group 2; [c] $P<0.05$ vs group.

Table 2. Incidence and Multiplicity of Invasive Adenocarcinoma (Experiment 2)

Group	No. of rats	Lateral		Ventral		Dorsal		Anterior	
		Incidence (%)	No. of foci	Incidence (%)	No. of foci	Incidence (%)	No. of foci	Incidence (%)	No. of foci
1	9	8 (89)	1.78 ± 1.10	8 (89)	4.22 ± 2.59**	2 (22)	0.44 ± 1.01	6 (67)	1.11 ± 1.05
2	9	7 (78)	1.67 ± 1.41	5 (56)	0.89 ± 0.93	0	-	7 (78)	0.78 ± 0.44
3	6	5 (83)	3.17 ± 1.72	2 (33)	0.33 ± 0.52	0	-	1 (17)	0.17 ± 0.41

** $P<0.01$ vs groups 2 and 3.

by intermittent TP administration (group 1 in experiment 2, shown in Fig. 1). The invasive carcinomas induced simulate human prostate cancer in several respects, such as perineural invasion and multicentric lesion development. To investigate mechanisms of prostate cancer progression, we previously combined administration of both DMAB and TP[5]. While several experiments were conducted with the aim of increasing the incidence of invasive cancer and shortening

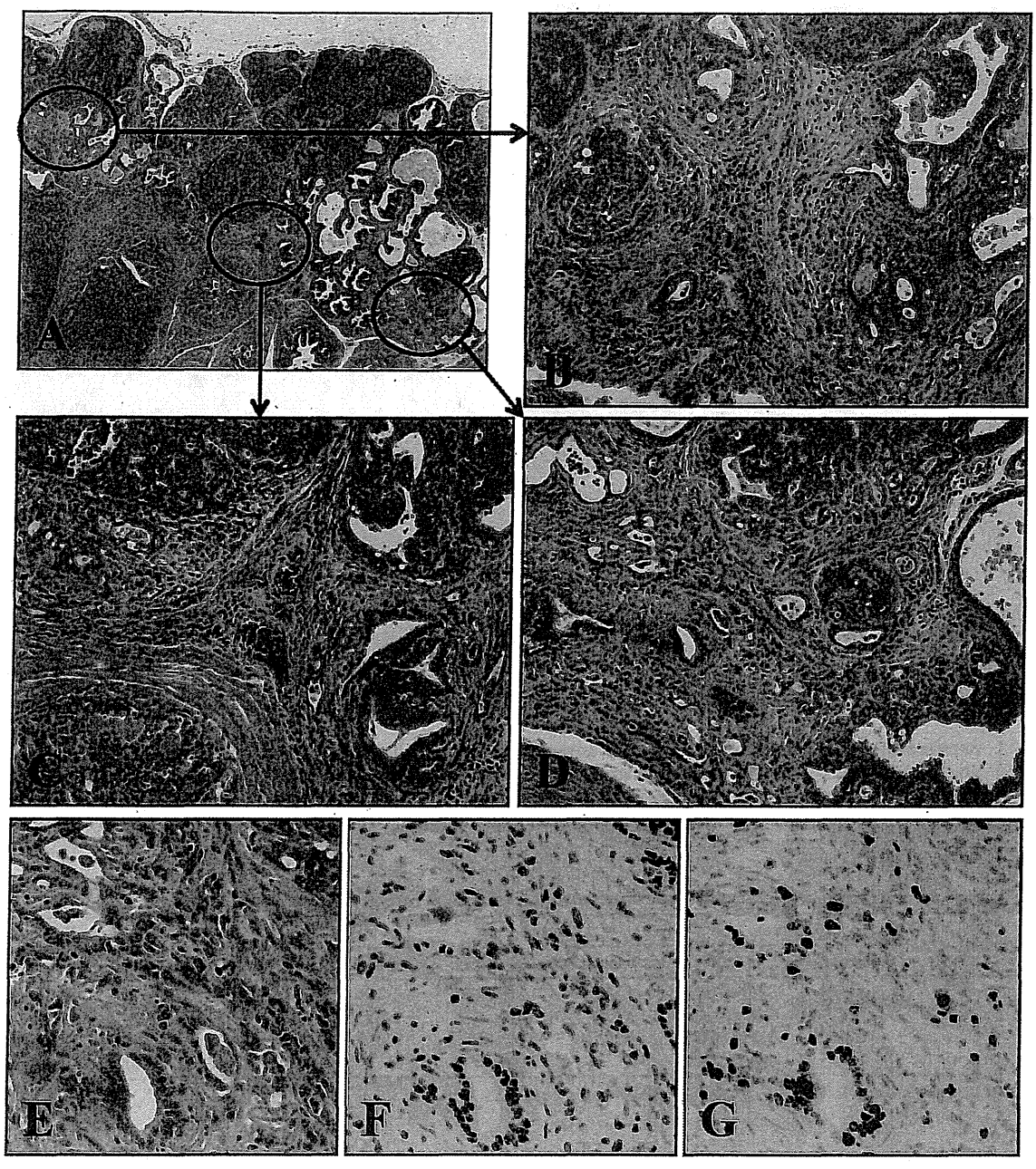

Fig. 3. Multicentric development of invasive adenocarcinomas in the lateral prostate in group 1 at week 15 after the beginning of experiment 2 (A–D). High magnifications of invasive adenocarcinoma with H&E (E), AR (F) and Ki-67 (G) staining.

the experimental period, none exceeded the DMAB + TP model in terms of the cancer incidence[13–16]. The new prostate carcinogenesis model documented here is characterized by invasive adenocarcinoma development at a high incidence in a short period without carcinogen administration. This rat model should enable us to investigate candidate chemopreventive agents for therapeutic effects as well as chemopreventive properties against prostate cancer.

We found that invasive adenocarcinoma incidences became greater as we increased the TP administration/withdrawal cycles for the TRAP rats. In our previous studies, testosterone induced invasive prostate adenocarcinomas in a dose- or duration-dependent manner after prostatic carcinogen treatment[14, 15]. However, continuous administration of testosterone alone earlier proved unable to cause development of invasive cancer with abundant reactive stromal tissue in the TRAP model[6,11]. The present results thus lead us to speculate that physiological destruction of the normal

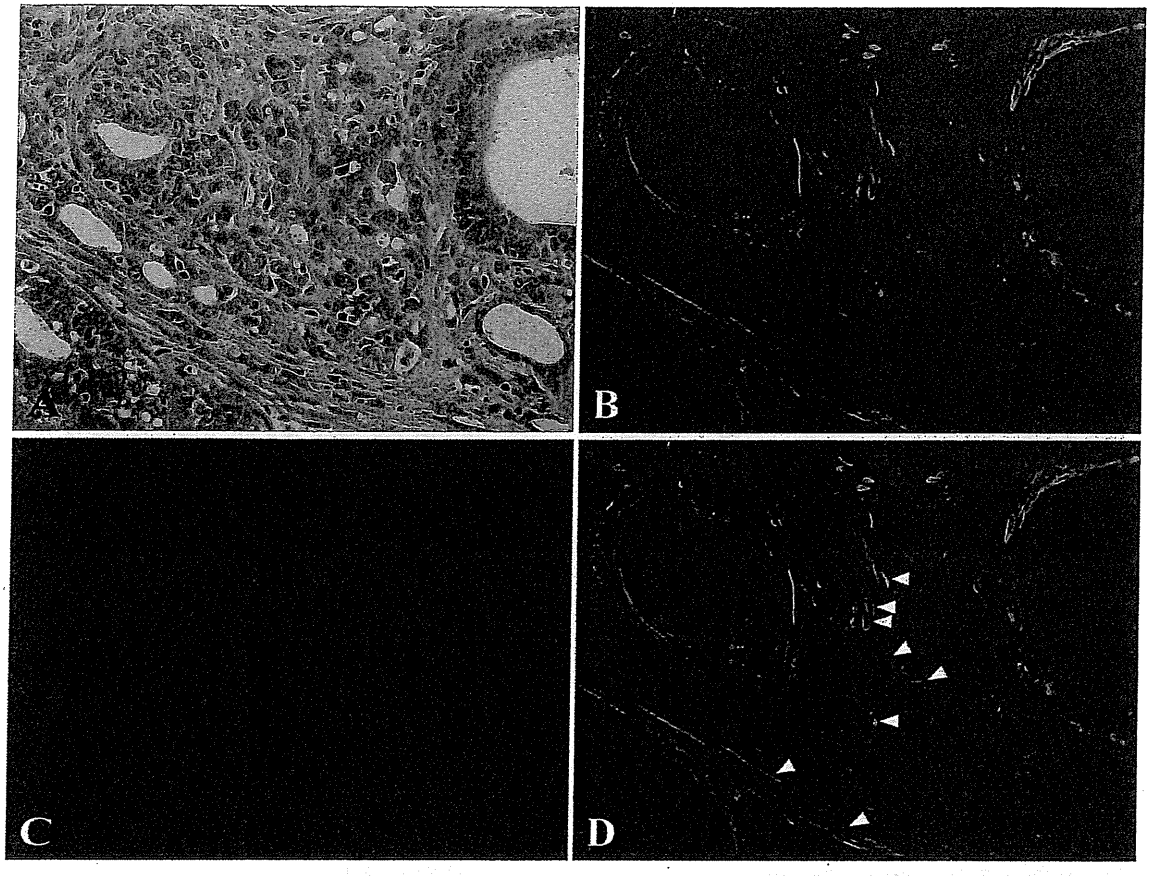

Fig. 4. Immunofluorescence analysis of an invasive adenocarcinoma in a lateral prostate. H&E (A). Immunofluorescence for smooth muscle actin (green, B) and vimentin (red, C), and a merged image (D). Blue, DAPI. Myofibroblasts coexpressing smooth muscle actin and vimentin are indicated by the arrowhead in (D).

acinar structure with stromal cell proliferation by androgen depletion plays an important role in the induction of invasive adenocarcinomas.

The process of primary cancer invasion, which initiates metastasis, is multifactorial and multistep and requires alteration of cell adherence, proteolytic degradation of extracellular matrix elements and tumor cell migration through tissue. Accumulating evidence has shown that stromal-epithelial interactions play critical roles in cancer progression[17–19]. The reactive tumor stroma mainly composed of cancer-associated fibroblasts (CAFs) including myofibroblasts, which are the predominant subpopulation of CAFs, is known to contribute to cancer development and progression[18–20]. Growth of myofibroblasts is reported to be stimulated by androgen[21]. TGFβ is one of the growth factors overexpressed in the prostate of rats after androgen ablation by orchiectomy[22]. TGFβ1 induces reactive oxygen species production via enhancement of NOX4 expression and may underly fibroblast-to-myofibroblast differentiation in the prostatic stroma[23], while myofibroblasts per se contribute to the production and activation of TGFβ1 and stromal cell-derived factor-1 (SDF-1)/CXCL12 by autocrine signaling loops[24]. Phosphoglycerate kinase-1 (PGK1), a downstream molecule of CXCL12-CXCR4 signaling, is upregulated in myofibroblasts, and this is involved in the enhanced proliferation and invasion of prostate cancer cells through activation of MMP, AKT and ERK pathways[25].

In conclusion, TP administration/withdrawal cycles appear to be of paramount importance to induction of invasive adenocarcinomas in the TRAP rat prostate. Our new rat prostate carcinogenesis model for invasive adenocarcinoma should provide opportunities to investigate molecular mechanisms of prostate cancer progression and may serve as a useful preclinical model for evaluating *in vivo* efficacy of preventive and therapeutic agents in terms of the tumor microenvironment.

Disclosure statement: The authors have no conflicts of interest.

Acknowledgments: This work was supported by a Grant-in-Aid for Cancer Research from the Ministry of Health, Labour and Welfare of Japan and a grant from the Society for Promotion of Pathology of Nagoya, Japan. The authors have no conflicts of interest regarding this research.

References

1. Siegel R, Naishadham D, and Jemal A. Cancer statistics, 2013. CA Cancer J Clin. **63**: 11–30. 2013. [Medline] [CrossRef]
2. Matsuda T, Marugame T, Kamo K, Katanoda K, Ajiki W, and Sobue T. Cancer incidence and incidence rates in Japan in 2006: Based on data from 15 population-based cancer registries in the monitoring of cancer incidence in Japan (MCIJ) project. Jpn J Clin Oncol. **42**: 139–147. 2012. [Medline] [CrossRef]
3. Zhang J, Dhakal IB, Zhao Z, and Li L. Trends in mortality from cancers of the breast, colon, prostate, esophagus, and stomach in East Asia: role of nutrition transition. Eur J Cancer Prev. **21**: 480–489. 2012. [Medline] [CrossRef]
4. Shirai T, Fukushima S, Ikawa E, Tagawa Y, and Ito N. Induction of prostate carcinoma in situ at high incidence in F344 rats by a combination of 3,2'-dimethyl-4-aminobiphenyl and ethinyl estradiol. Cancer Res. **46**: 6423–6426. 1986. [Medline]
5. Shirai T, Tamano S, Kato T, Iwasaki S, Takahashi S, and Ito N. Induction of invasive carcinomas in the accessory sex organs other than the ventral prostate of rats given 3,2'-dimethyl-4-aminobiphenyl and testosterone propionate. Cancer Res. **51**: 1264–1269. 1991. [Medline]
6. Asamoto M, Hokaiwado N, Cho YM, Takahashi S, Ikeda Y, Imaida K, and Shirai T. Prostate carcinomas developing in transgenic rats with SV40 T antigen expression under probasin promoter control are strictly androgen dependent. Cancer Res. **61**: 4693–4700. 2001. [Medline]
7. Seeni A, Takahashi S, Takeshita K, Tang M, Sugiura S, Sato SY, and Shirai T. Suppression of prostate cancer growth by resveratrol in the transgenic rat for adenocarcinoma of prostate (TRAP) model. Asian Pac J Cancer Prev. **9**: 7–14. 2008. [Medline]
8. Takahashi S, Takeshita K, Seeni A, Sugiura S, Tang M, Sato SY, Kuriyama H, Nakadate M, Abe K, Maeno Y, Nagao M, and Shirai T. Suppression of prostate cancer in a transgenic rat model via gamma-tocopherol activation of caspase signaling. Prostate. **69**: 644–651. 2009. [Medline] [CrossRef]
9. Takahashi S, Uemura H, Seeni A, Tang M, Komiya M, Long N, Ishiguro H, Kubota Y, and Shirai T. Therapeutic targeting of angiotensin II receptor type 1 to regulate androgen receptor in prostate cancer. Prostate. **72**: 1559–1572. 2012. [Medline] [CrossRef]
10. Long N, Suzuki S, Sato S, Naiki-Ito A, Sakatani K, Shirai T, and Takahashi S. Purple corn color inhibition of prostate carcinogenesis by targeting cell growth pathways. Cancer Sci. **104**: 298–303. 2013. [Medline] [CrossRef]
11. Cho YM, Takahashi S, Asamoto M, Suzuki S, Inaguma S, Hokaiwado N, and Shirai T. Age-dependent histopathological findings in the prostate of probasin/SV40 T antigen transgenic rats: lack of influence of carcinogen or testosterone treatment. Cancer Sci. **94**: 153–157. 2003. [Medline] [CrossRef]
12. Cho YM, Takahashi S, Asamoto M, Suzuki S, Tang M, and Shirai T. Suppressive effects of antiandrogens, finasteride and flutamide on development of prostatic lesions in a transgenic rat model. Prostate Cancer Prostatic Dis. **10**: 378–383. 2007. [Medline] [CrossRef]
13. Shirai T, Imaida K, Masui T, Iwasaki S, Mori T, Kato T, and Ito N. Effects of testosterone, dihydrotestosterone and estrogen on 3,2'-dimethyl-4-aminobiphenyl-induced rat prostate carcinogenesis. Int J Cancer. **57**: 224–228. 1994. [Medline] [CrossRef]
14. Shirai T, Sano M, Imaida K, Takahashi S, Mori T, and Ito N. Duration dependent induction of invasive prostatic carcinomas with pharmacological dose of testosterone propionate in rats pretreated with 3,2'-dimethyl-4-aminobiphenyl and development of androgen-independent carcinomas after castration. Cancer Lett. **83**: 111–116. 1994. [Medline] [CrossRef]
15. Shirai T, Tamano S, Sano M, Imaida K, Hagiwara A, Futakuchi M, Takahashi S, and Hirose M. Site-specific effects of testosterone propionate on the prostate of rat pretreated with 3,2'-dimethyl-4-aminobiphenyl: dose-dependent induction of invasive carcinomas. Jpn J Cancer Res. **86**: 645–648. 1995. [Medline] [CrossRef]
16. Cui L, Mori T, Takahashi S, Imaida K, Akagi K, Yada H, Yaono M, and Shirai T. Slight promotion effects of intermittent administration of testosterone propionate and/or diethylstilbestrol on 3,2'-dimethyl-4-aminobiphenyl-initiated rat prostate carcinogenesis. Cancer Lett. **122**: 195–199. 1998. [Medline] [CrossRef]
17. Valastyan S, and Weinberg RA. Tumor metastasis: molecular insights and evolving paradigms. Cell. **147**: 275–292. 2011. [Medline] [CrossRef]
18. Barron DA, and Rowley DR. The reactive stroma microenvironment and prostate cancer progression. Endocr Relat Cancer. **19**: R187–R204. 2012. [Medline] [CrossRef]
19. Otranto M, Sarrazy V, Bonte F, Hinz B, Gabbiani G, and Desmouliere A. The role of the myofibroblast in tumor stroma remodeling. Cell Adh Migr. **6**: 203–219. 2012. [Medline] [CrossRef]
20. Orimo A, and Weinberg RA. Heterogeneity of stromal fibroblasts in tumors. Cancer Biol Ther. **6**: 618–619. 2007. [Medline] [CrossRef]
21. Webber MM, Trakul N, Thraves PS, Bello-DeOcampo D, Chu WW, Storto PD, Huard TK, Rhim JS, and Williams DE. A human prostatic stromal myofibroblast cell line WPMY-1: a model for stromal-epithelial interactions in prostatic neoplasia. Carcinogenesis. **20**: 1185–1192. 1999. [Medline] [CrossRef]
22. Desai KV, and Kondaiah P. Androgen ablation results in differential regulation of transforming growth factor-β isoforms in rat male accessory sex organs and epididymis. J Mol Endocrinol. **24**: 253–260. 2000. [Medline] [CrossRef]
23. Sampson N, Koziel R, Zenzmaier C, Bubendorf L, Plas E, Jansen-Durr P, and Berger P. ROS signaling by NOX4 drives fibroblast-to-myofibroblast differentiation in the diseased prostatic stroma. Mol Endocrinol. **25**: 503–515. 2011. [Medline] [CrossRef]
24. Kojima Y, Acar A, Eaton EN, Mellody KT, Scheel C, Ben-Porath I, Onder TT, Wang ZC, Richardson AL, Weinberg RA, and Orimo A. Autocrine TGF-β and stromal cell-derived factor-1 (SDF-10 signaling drives the evolution of tumor-promoting mammary stromal myofibroblasts. Proc Natl Acad Sci USA. **107**: 20009–20014. 2010. [Medline] [CrossRef]
25. Wang J, Ying G, Wang J, Jung Y, Lu J, Zhu J, Pienta KJ, and Taichman RS. Characterization of phosphoglycerate kinase-1 expression of stromal cells derived from tumor microenvironment in prostate cancer progression. Cancer Res. **70**: 471–480. 2010. [Medline] [CrossRef]

Rev Endocr Metab Disord (2013) 14:207–216
DOI 10.1007/s11154-013-9242-z

The role of endothelial insulin signaling in the regulation of glucose metabolism

Tetsuya Kubota · Naoto Kubota · Takashi Kadowaki

Published online: 16 April 2013

Abstract The skeletal muscle is one of the major target organs of insulin and plays an essential role in insulin-induced glucose uptake. Some evidence indicates that insulin delivery to skeletal muscle interstitium through the endothelial cells is the rate-limiting step in insulin-stimulated glucose uptake. Researchers have also found that this process is impaired by insulin resistance in type 2 diabetes and obesity. A recent study of ours demonstrated that insulin signaling in the endothelial cells plays a pivotal role in the regulation of glucose uptake by the skeletal muscle. Specifically, impaired insulin signaling in the endothelial cells, with reduction of insulin-induced eNOS phosphorylation, causes attenuation of the insulin-induced capillary recruitment and insulin delivery, which, in turn reduces glucose uptake by the skeletal muscle in high-fat diet-fed mice. Moreover, restoration of the insulin-induced eNOS phosphorylation in the endothelial cells completely reverses the reduction in the capillary recruitment and insulin delivery, and as a result, significantly restores glucose uptake by the skeletal muscle. In the present review, we describe the recent progress in research on the physiological and pathophysiological roles of endothelial insulin signaling in the regulation of insulin-induced glucose uptake by the skeletal muscle.

Keywords Insulin signaling · Endothelial cell · Capillary recruitment · Skeletal muscle insulin resistance · Endothelial nitric oxide synthase · Insulin transport

1 Introduction

In recent years there has been a rapid growth in the incidence of type 2 diabetes in both Western and Asian countries [1, 2]. The increasing incidence of type 2 diabetes is most likely due to genetic factors and pathological processes among the ageing population exposed to negative health effects of certain lifestyle, including diets high in fat combined with reduced levels of exercise [1]. Type 2 diabetes magnifies the risk of cardiovascular mortality, which is corollary to a growing epidemic of micro- and macro-vascular complications, including diabetic nephropathy and coronary artery disease [3, 4]. Moreover, high prevalence of type 2 diabetes is associated with a significant economic burden [5]. It is important to elucidate the precise molecular mechanisms underlying the development and progression of type 2 diabetes.

Skeletal muscle plays an essential role in the maintenance of normal blood glucose concentrations and is one of the major sites of insulin resistance in type 2 diabetic patients [6]. Excess lipid storage in adipose tissue leads to accumulation of intracellular lipid derivatives (diacylglycerol and ceramides), inflammation and oxidative stress in the skeletal muscle. As a result, intramyocellular insulin signaling is impaired, thereby causing skeletal muscle insulin resistance [7–10]. The impairment of insulin intracellular signaling pathways within the myocytes caused by ectopic fat accumulation is considered to be a major mechanism underlying skeletal muscle insulin resistance (Fig. 1a). These researches are comprehensively reviewed elsewhere [11, 12].

On the other hand, in order to stimulate insulin-induced glucose uptake by the skeletal muscle, insulin has to be

Tetsuya Kubota and Naoto Kubota contributed equally to this work.

T. Kubota · N. Kubota (✉) · T. Kadowaki (✉)
Department of Diabetes and Metabolic Diseases, Graduate School of Medicine, University of Tokyo, 7-3-1 Hongo, Bunkyo-ku, Tokyo 113-8655, Japan
e-mail: nkubota-tky@umin.ac.jp
e-mail: kadowaki-3im@h.u-tokyo.ac.jp

T. Kubota · N. Kubota
Clinical Nutrition Program, National Institute of Health and Nutrition, Tokyo 162-8636, Japan

N. Kubota · T. Kadowaki
Translational Systems Biology and Medicine Initiative (TSBMI), University of Tokyo, Tokyo 153-8515, Japan

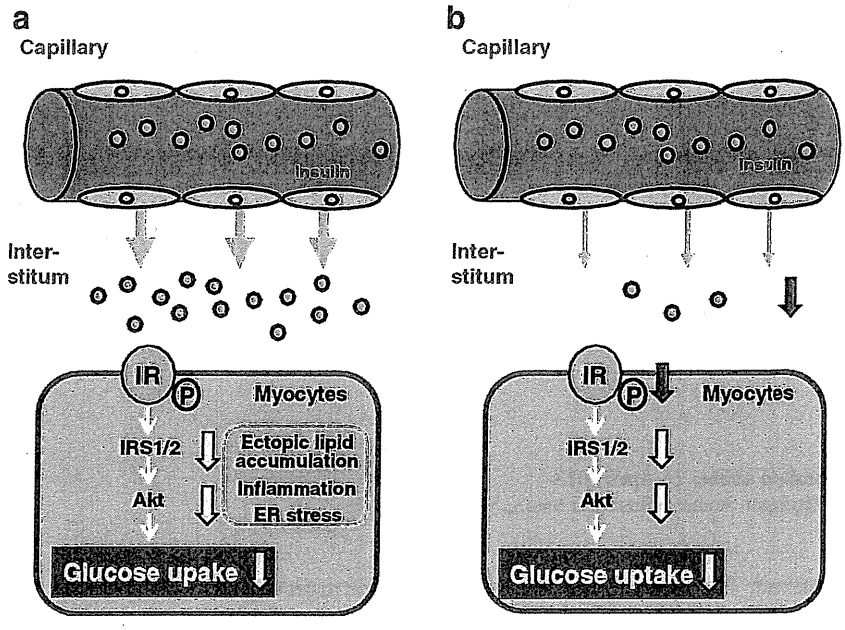

Fig. 1 Two models of skeletal muscle insulin resistance. a Impairment of cellular signaling within the myocytes. b Impairment of insulin delivery to skeletal muscle

delivered into the capillaries and cross the endothelial barrier to enter the interstitial spaces [13]. Some evidence indicates that insulin delivery to skeletal muscle interstitium through the endothelial cells is the rate-limiting step in insulin-stimulated glucose uptake by the skeletal muscle and that this process is impaired in insulin resistance with type 2 diabetes and obesity [14–16]. In addition to an impairment of cellular signaling within the myocytes, there is an impairment of insulin delivery to skeletal muscle as a major mechanism underlying skeletal muscle insulin resistance (Fig. 1b).

In this review, we describe recent progress in research on the physiological and pathophysiological roles of endothelial insulin signaling in the regulation of insulin-induced glucose uptake by the skeletal muscle.

2 Insulin action in the endothelial cells

There are two major pathways in insulin signaling of endothelial cells: phosphoinositide 3 (PI3) kinase-Akt and RAS-mitogen activated protein (MAP) kinase pathway [17, 18].

Insulin action is initiated by the binding of the insulin molecule to its specific cell surface receptor [19]. Insulin binding to its receptor results in the tyrosine phosphorylation of the insulin receptor substrate (IRS) by the insulin receptor tyrosine kinase. Although the IRS family is represented by IRS-1, 2, 3, 4, 5 and 6 [20], IRS-1 and 2 are particularly important in endothelial cells [21, 22]. Phosphorylated IRSs allow association of IRSs with the regulatory subunit of PI3 kinase. PI3 kinase activates 3-phosphoinositide-dependent protein kinase 1 (PDK1), which activates Akt, a serine kinase. Akt directly phosphorylates eNOS at Ser1177, resulting in increased eNOS activity and nitric oxide (NO) production [23–25]. NO mediates vasodilation mainly by diffusion to vascular smooth muscle cells, where it activates soluble guanylate cyclase, resulting in the formation of cyclic guanosine monophosphate (cGMP) [26, 27].

In addition to eNOS activation, insulin signaling in the endothelial cells regulates vasoconstrictor endothelin (ET)-1 expression [28, 29]. Insulin activates IR and allows binding of the intracellular mediator Shc to the Src homology 2 domain of growth factor receptor-bound protein 2 (Grb2). This, in turn, leads to activation of the Son of Sevenless (SOS) and Ras, which then initiates a kinase phosphorylation cascade involving Raf, MAP kinase kinase pathway [30]. Activation of the MAP kinase induces the secretion of ET-1. The secreted ET-1 binds to its receptor, ET-1_A and ET-1_B, and activates PKC in vascular smooth muscle cells. PKC activation by ET-1 leads to contraction in the vascular smooth muscle cells [31]. A MAP kinase inhibitor completely suppressed insulin-stimulated ET-1 expression, although pretreatment with wortmannin, a PI3 kinase inhibitor, did not significantly affect insulin-stimulated ET-1 expression [32].

Two major pathways of insulin signaling in endothelial cells regulate distinct biological functions. A critical balance between endothelium-derived relaxing and contracting factors maintains vascular homeostasis.

3 Selective insulin resistance of endothelial cells in obese models

Interestingly, PI3 kinase-Akt pathway alone is impaired in the endothelial cells of obese and type 2 diabetes models [33, 34]. King and colleagues found the activity of IRS-2

associated PI3 kinase was impaired in the vasculature of obese Zucker rats [35]. On the other hand, the MAP kinase pathway remains unchanged in the vasculature [36]. Jansson and colleagues reported that in microvascular endothelial cells isolated from type 2 diabetes subjects, the phosphorylation of Akt in response to insulin attenuated, whereas insulin-stimulated phosphorylation of extracellular signal-related kinase (ERK)1/2 was increased [37]. In reference to these phenomena, King has coined the phrase 'selective insulin resistance' of endothelial cells in obese models [27].

Why is only the PI3 kinase pathway of endothelial cells impaired in obesity? IRS-2 expression levels dropped markedly in the endothelial cells of both ob/ob and high-fat (HF) diet-fed mice, although ET-1 expression remained unchanged [38]. To elucidate the mechanisms by which the expression of IRS-2 was downregulated, we conducted an experiment using human umbilical arterial endothelial cells (HUAEC). The expression of IRS-2 was significantly suppressed from 3 h onwards after insulin treatment. The promoter region of the IRS-2 gene contains an insulin response element, which is recognised by forkhead transcription factor O1 (FoxO1) [39, 40]. To investigate the relationship between IRS-2 and FoxO1, endothelial cells were immunostained with FoxO1 antibody after insulin treatment. The expression of IRS-2 was significantly suppressed in parallel with FoxO1 translocation from the nuclei to the cytosol, and the expression was restored by treatment with LY294002, a PI3 kinase inhibitor. Moreover, transfection of constitutively active FoxO1 (C/A-FoxO1) restored the insulin-induced suppression of IRS-2. These data suggest that hyperinsulinemia may lead to a decrease of IRS-2-PI3kinase-Akt pathway in the endothelial cells in mouse models of obesity (Fig. 2).

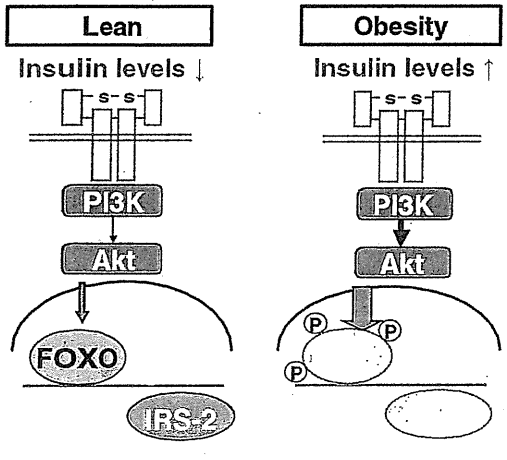

Fig. 2 Hyperinsulinemia is one of the mechanisms underlying the decrease in the expression of endothelial IRS-2 in obesity. In lean subject, expression levels of IRS-2 increased through FoxO1 activation. In contrast, hyperinsulinemia observed in obesity is reduced IRS-2 expression through PI3kinase-Akt-FoxO1 pathway in the endothelial cells

4 Insulin delivery to skeletal muscle is the rate-limiting step in insulin-induced glucose uptake by the skeletal muscle

Insulin, secreted by pancreatic β cells, has to be delivered to skeletal muscle to ensure a supply of insulin to myocytes. Using the compartmental model in the 1970s, Andres and colleagues indicated that insulin was distributed more slowly to the compartment 3 corresponding to skeletal muscle than to other compartments, such as plasma and liver, and that the time-course of insulin equilibration with this pool closely paralleled the glucose infusion rate [41, 42]. Furthermore, the dynamics of insulin concentrations in the skeletal muscle lymphatics, which was derived from the interstitial fluid in the skeletal muscle, was actually slow, and was significantly correlated with the peripheral glucose uptake after insulin infusion [14]. On the other hand, injection of insulin directly into the interstitium of the skeletal muscle was followed by a prompt increase in glucose uptake [43]. It showed a strong correlation between the interstitial insulin concentration and the increase in the glucose uptake by the skeletal muscle.

Moreover, in obese and type 2 diabetes subjects, although insulin distribution to the plasma and liver did not differ significantly, that of skeletal muscle was significantly impaired, and insulin-induced glucose uptake was further delayed in the skeletal muscle as compared with normal subjects [44, 45]. Consistent with these findings, in obese subjects, the appearance and concentrations of insulin in the interstitial fluid of the skeletal muscle were found to be significantly delayed and decreased as compared with control subjects [46]. These findings indicate that insulin delivery to the skeletal muscle is the rate-limiting step in the insulin-induced glucose uptake (Fig. 3). Two discrete steps have been reported for the mechanism regulating insulin delivery to the skeletal muscle: an increase in the trans-endothelial transport of insulin and an increase in the available capillary surface area (capillary recruitment).

5 Insulin delivery to the skeletal muscle

5.1 Trans-endothelial transport of insulin

There is a difference between the types of capillaries in the liver and those in the skeletal muscle. It is thought that the occluded junctions of the endothelial cells of the capillaries in the skeletal muscle may prevent paracellular transport of most macromolecules, including insulin, whereas the fenestrated endothelium of the capillaries in the liver freely permits paracellular passage of macromolecules [47]. In fact, a more rapid insulin action kinetics has been observed in the liver than in the skeletal muscle [16].

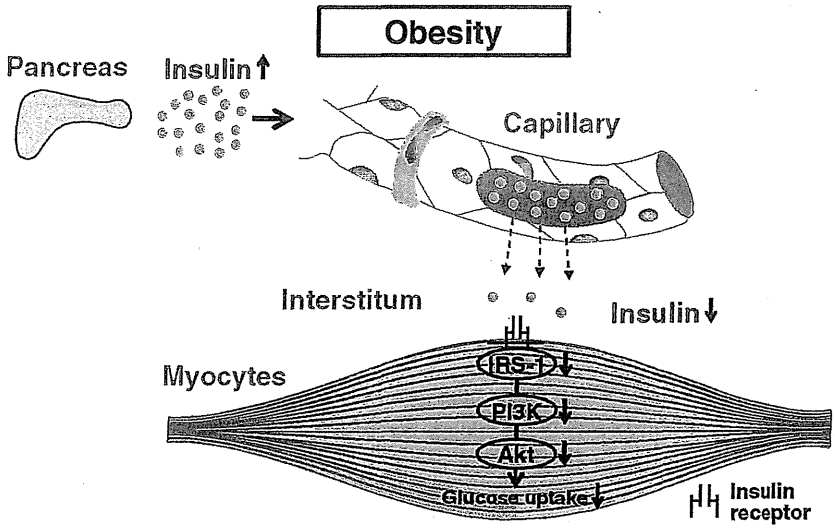

Fig. 3 Insulin delivery to the skeletal muscle is the rate-limiting step in the insulin-induced glucose uptake. The appearance and concentrations of insulin in the interstitial fluid of the skeletal muscle is significantly delayed and decreased in obesity

What mechanisms are involved in trans-endothelial transport of continuous capillaries? There are two different pathways: insulin receptor mediated and non-insulin receptor mediated. King and Johnson reported that the trans-endothelial movement of insulin was saturable in the cultured endothelial cells. This movement was blocked by antibodies against the insulin receptor [48]. Some studies subsequently supported these data *in vitro* [49, 50]. These findings suggest that movement of insulin across the endothelial cells, at least *in vitro*, is insulin receptor-mediated.

In addition to the insulin receptor-mediated pathway, Bergman and colleagues reported that when physiological and pharmacological (very high) levels of insulin were injected into dogs, the steady-state plasma/interstitium gradient was reduced more markedly at the pharmacological rather than physiological insulin level [51]. Moreover, the appearance of the insulin analogue NN304 in dog skeletal muscle interstitial fluid was constant even when sufficient insulin was injected to saturate the endothelial insulin receptors [52]. These data suggest that movement of insulin into skeletal muscle interstitium *in vivo* may partly occur via a non-saturable process such as passive diffusion via a paracellular or transcellular pathway.

Barrett and colleagues measured the rate of ^{125}I-insulin uptake by rat hindlimb muscle for an extremely short period of time (5 min), when unlabelled insulin was infused continuously by hyperinsulinemic-uglycemic clamp. The unlabelled insulin significantly reduced the clearance of ^{125}I-insulin in plasma after 5 min [53, 54]. This observation suggests that the transendothelial movement of insulin is involved in insulin receptor-mediated pathway *in vivo*. Moreover, they noted that when fluorescent-tagged insulin was injected into the rat, the insulin receptor and caveolae were colocalized [55]. Since caveolae had already been implicated in the transcytosis of albumin and other proteins, Wang et al. investigated *in vitro* whether caveolin-1 is required for the transendothelial transport of insulin. Knockdown of caveolin-1 reduced FITC-insulin uptake in bovine aortic endothelial cells. Furthermore, IL-6 or tumour necrosis factor (TNF)α inhibited FITC-insulin uptake as well as the expression of caveolin-1 mRNA and protein [56]. However, systemic caveolae knockout mice showed increased passive diffusion via a paracellular or transcellular pathway [57]. It is still unclear whether insulin receptor-mediated and non-insulin receptor-mediated pathways may be related to each other or may function independently in the physiological and pathophysiological states *in vivo*. A great deal more work needs to be done in order to understand the regulation of this process.

5.2 Insulin regulates capillary recruitment

In 1997, Rattigan and colleagues first showed direct evidence for insulin-mediated capillary recruitment by using 1-methylxathine (1-MX) [58], which has no vasoactivity and is converted solely to 1-methylurate by xanthine oxidase. Xanthine oxidase exists primarily in the endothelial cells of capillaries, but not large vessels [59]. Therefore, 1-MX provides an effective tool for determining capillary recruitment. Using this method, they demonstrated that insulin increased both 1-MX metabolism and glucose uptake in rat hindlimb. However, the clearance of 1-MX by human capillaries is lower than in the rodent, presumably because of lower content of xanthine oxidase [54, 60]. This method could not be adapted to human studies. Barrett and colleagues adapted a contrast enhanced ultrasound (CEU) method that had been extensively used in cardiac muscle [61, 62]. Using this technique, they found that capillary recruitment was significantly enhanced within 30 min of insulin infusion, and this was of similar magnitude to the changes observed at 90 min. On the other hand, an increase of blood flow was observed 120 min after insulin infusion [63]. These data

indicate that insulin-induced capillary recruitment preceded the increase in total blood flow.

In our experimental results of normal mice, although capillary recruitment was observed 10 min after insulin infusion, no such increase was observed in the interstitial insulin concentration. An increase of the interstitial concentrations of insulin was observed 60 min after insulin infusion. Consistent with the results for the interstitial concentrations of insulin, the phosphorylation levels of Akt in the skeletal muscle were increased 60 min after insulin infusion. [38]. These data, along with careful studies by Miles [16], demonstrate that capillary recruitment increases slowly, followed by interstitial insulin concentration and tyrosine phosphorylation of the skeletal muscle insulin receptor, whereas plasma insulin levels rise immediately after the insulin infusion. However, 2 h or more is typically required to see the effects of insulin on blood flow.

5.2.1 Insulin signaling in the endothelial cells regulates capillary recruitment

Endothelium-derived NO is known to mediate insulin-induced microvascular perfusion in skeletal muscle in animals and humans [38, 64–66]. In fact, eNOS knockout mice showed impaired insulin-induced capillary recruitment in the skeletal muscle [38, 64]. N-monomethyl-L-arginine (L-NMMA), an NO synthase (NOS) inhibitor, blocked capillary recruitment in response to insulin in the skeletal muscle [65]. Moreover, inhibiting NOS diminished insulin-induced capillary recruitment in the skeletal muscle in humans [66]. This finding suggests that capillary recruitment is regulated in an NO-dependent manner. The correlations between insulin signaling in the endothelial cells and capillary recruitment in the skeletal muscle were elucidated in the endothelial-cell-specific IRS-2 knockout (ETIRS2KO) mice. The insulin-induced eNOS phosphorylation, capillary recruitment and increases of interstitial concentrations of insulin were impaired in the ETIRS2KO mice. Furthermore, decreased insulin-induced glucose uptake by the skeletal muscle was observed in the ETIRS2KO mice after insulin infusion. Consistent with these results, the phosphorylation levels of Irβ in the skeletal muscle were also decreased in the ETIRS2KO mice after insulin infusion [38]. These data suggest that IRS-2 deletion in the endothelial cells causes an insulin signaling defect in the cells that results in impairment of insulin-induced eNOS activation, capillary recruitment and increase of the interstitial concentrations of insulin, consequently impairing the skeletal muscle glucose uptake. Some evidence indicates that IRS-1, as well as IRS-2, may play an important role in the endothelial cells. The activation of Jun N-terminal protein kinase (JNK) by IL-6 increased IRS-1 serine phosphorylation resulting in impairment of the vasodilator effects of insulin [67]. Moreover, insulin-stimulated Akt and eNOS activation were impaired in cultured human endothelial cells carrying the IRS-1 gene G972R variant, which is associated with an impairment of the ability of IRS-1 to recruit the p85 regulatory subunit of PI3 kinase [68]. The role of IRS-1 expressed in the endothelial cells in the regulation of insulin-induced glucose uptake by the skeletal muscle was investigated using the endothelial-cell-specific IRS-1 knockout (ETIRS1KO) mice. The insulin-stimulated phosphorylation levels of Akt or eNOS in the ETIRS1KO mice remained unchanged. ETIRS1KO mice did not show skeletal muscle insulin resistance. Moreover, endothelial-cell-specific IRS-1/IRS-2 double-knockout (ETIRS1/2DKO) mice were used to address the role of IRS-1 and IRS-2 in the endothelial cells. The insulin-stimulated phosphorylation of Akt and eNOS were almost completely abolished in the ETIRS1/2DKO mice. Insulin-induced glucose uptake by the skeletal muscle in the ETIRS1/2DKO mice was reduced as compared with the values not only in the control mice, but also in the ETIRS2KO mice [38]. These data suggest that IRS-1 may play a significant role in endothelial cell insulin signaling. This becomes evident especially when IRS-2 expression is downregulated, such as in the ETIRS2KO and HF diet-fed mice.

5.2.2 eNOS activation increases insulin-induced capillary recruitment and glucose uptake by the skeletal muscle

To determine whether restoration of the insulin-induced eNOS phosphorylation in the endothelial cells might restore the glucose uptake by the skeletal muscle, beraprost sodium (BPS), a stable prostaglandin $(PGI)_2$ analogue [69], was administered to the ETIRS2KO mice. This agent has been reported to increase the expression levels of eNOS mRNA and protein through the cyclic adenosine monophosphate (cAMP)-, protein kinase A- and cAMP-responsive element-mediated pathways [70], and is clinically used for the treatment of peripheral artery disease and primary pulmonary hypertension [71, 72]. Indeed, this treatment increased the eNOS mRNA and protein expression levels in the endothelial cells. BPS treatment restored insulin-induced phosphorylation of eNOS in the ETIRS2KO mice. The insulin-induced capillary recruitment and increase of interstitial concentrations of insulin were restored in the BPS-treated ETIRS2KO mice. The restoration of the insulin-induced capillary recruitment by BPS treatment in the ETIRS2KO mice was completely blocked by administration of the NOS inhibitor, N^G-nitro-$_L$-arginine methyl ester ($_L$-NAME), suggesting that the restoration of the insulin-induced capillary recruitment by BPS treatment was NO-dependent. Moreover, glucose uptake by the skeletal muscle was completely restored in the BPS-treated ETIRS2KO mice. Consistent with the results for the interstitial insulin concentrations, the phosphorylation levels of Irβ in the skeletal muscle were also completely restored in the BPS-treated ETIRS2KO mice after insulin infusion [38].

NO-dependence has also been supported by the use of an agent other than BPS. Glucagon-like peptide 1(GLP-1),

which increased insulin secretion from the β cells and is clinically used for the treatment of type 2 diabetes [73], has been known to improve endothelial function [74–76]. Recently, Chai et al. reported that GLP-1 increased insulin-induced capillary recruitment and glucose uptake by the skeletal muscle in normal rats; these effects were abolished by L-NAME treatment [77]. These data suggest that eNOS activation in endothelial cells increases the insulin-induced capillary recruitment and interstitial concentrations of insulin, consequently promoting the insulin-induced glucose uptake by the skeletal muscle.

5.2.3 Insulin-induced capillary recruitment and glucose uptake by the skeletal muscle were impaired in obesity-related insulin resistance - effects restored by eNOS activation

Clark and colleagues reported that insulin resistance, generated either by infusion of free fatty acids [78], TNFα [79, 80], pharmacological blockade [81], or in obese Zucker rats [82], was accompanied by impairments in both insulin-induced capillary recruitment and glucose uptake by the skeletal muscle. There are also some data that indicate impairment of insulin-induced capillary recruitment in type 2 diabetes subjects [83–86]. In HF diet-fed mice, a series of changes in eNOS activation, capillary recruitment, interstitial concentrations of insulin and activation of the myocyte Akt after insulin infusion were carefully observed. Unlike in normal mice, eNOS activation and capillary recruitment were significantly impaired along with IRS-2 downregulation, presumably due to hyperinsulinemia and the significant decrease in the level of interstitial insulin in the HF diet-fed mice after insulin infusion. Consistent with the results for the interstitial concentrations of insulin, the phosphorylation levels of Akt and glucose uptake by the skeletal muscle also decreased in the HF diet-fed mice after insulin infusion [38]. These data suggest that the decreased eNOS activation appears to be involved along with the impaired insulin-induced capillary recruitment and increase

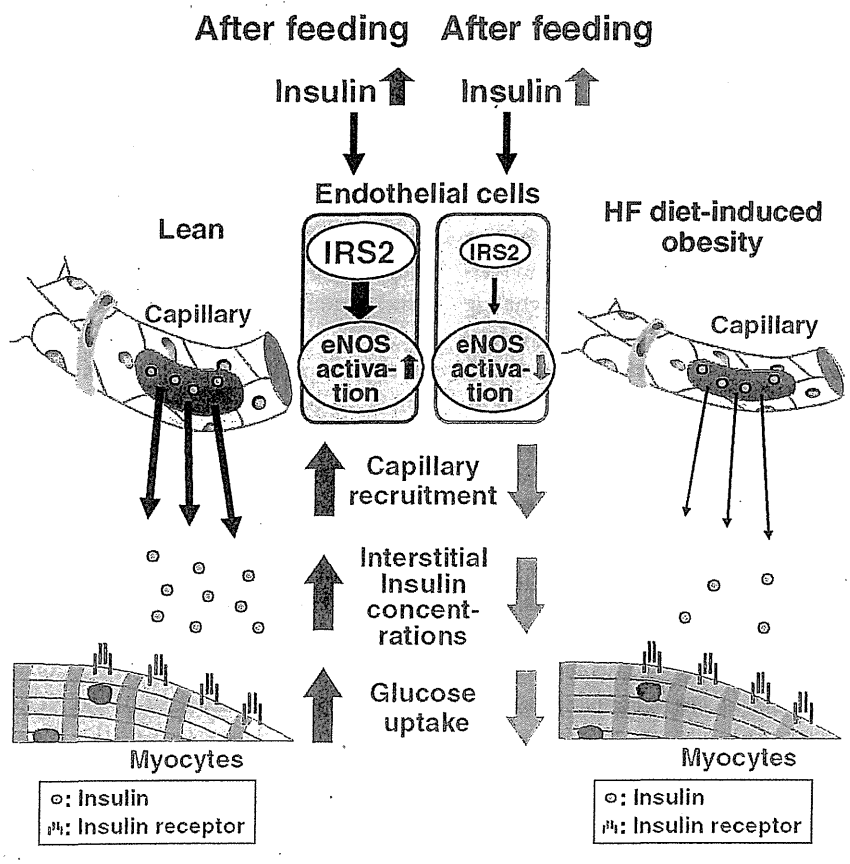

Fig. 4 Impaired insulin signaling in the endothelial cells reduces insulin-induced glucose uptake by the skeletal muscle in obese subjects. Since the plasma insulin levels of lean subjects are low, and the expression levels of IRS-2 in their endothelial cells are maintained under the fasting conditions, after feeding, insulin-mediated Akt and eNOS activations are induced optimally, resulting in insulin-induced capillary recruitment, increase of interstitial insulin concentrations, and glucose uptake by the skeletal muscle. By contrast, since downregulation of IRS-2 expression is induced by hyperinsulinemia in the endothelial cells of obese subjects, the insulin-mediated Akt and eNOS activations after feeding are inadequate, and as a result, insulin-induced capillary recruitment, increase of interstitial insulin concentrations, and glucose uptake by the skeletal muscle are impaired

of the interstitial concentrations of insulin in the impaired glucose uptake by the skeletal muscle in the HF diet-fed obese mice.

To investigate whether the restoration of insulin-induced eNOS phosphorylation in endothelial cells can equivalently ameliorate the impaired glucose uptake by the skeletal muscle in the HF diet-fed mice, BPS was administered to these mice. BPS treatment in the HF diet-fed mice restored insulin-induced phosphorylation of eNOS. The decreased capillary recruitment and interstitial concentrations of insulin observed in the HF diet-fed mice were restored after BPS treatment. NO-dependency was confirmed by the fact that the restoration of the capillary recruitment by BPS treatment in the HF diet-fed mice was completely blocked by L-NAME treatment. Consequently, the insulin-induced glucose uptake was significantly, but not completely, restored by BPS treatment. Consistent with the results for glucose uptake, the insulin-induced phosphorylation levels of Irβ in the skeletal muscle were significantly, but not completely, restored following BPS treatment in the HF diet-fed mice. The glucose uptake by the skeletal muscle isolated from HF diet-fed mice remained essentially unchanged after BPS treatment, indicating that BPS treatment does not mitigate the HF diet-induced impairment of glucose uptake by the skeletal muscle per se. This may explain why insulin-induced glucose uptake was not completely improved by BPS treatment, although both capillary recruitment and interstitial insulin concentration were completely restored by BPS treatment. Taken together, restoration of insulin-induced eNOS activation in endothelial cells restored the insulin-induced capillary recruitment and interstitial insulin concentrations, resulting in improvement of skeletal muscle glucose uptake in the HF diet-fed obese mice. Iloprost infusion, another PGI_2 analogue, improved insulin-stimulated whole-body glucose uptake in type 2 diabetes subject. Jansson et al. reported that the selective PDE-5 inhibitor tadalafil, which intensifies the effect of NO in smooth muscle cells [26, 87], improved capillary recruitment and forearm glucose uptake in insulin resistance with type 2 diabetes [88].

6 Conclusion

Recent studies have provided us with great insight into the mechanism of insulin resistance in skeletal muscle (Fig. 4). Since the plasma insulin levels of lean subjects are low, and the expression levels of IRS-2 in their endothelial cells are presumably maintained under the fasting condition, insulin-mediated Akt and eNOS activations are induced optimally after feeding, resulting in insulin-induced capillary recruitment, increase of interstitial insulin concentrations, and increase of glucose uptake by the skeletal muscle. In contrast, since downregulation of IRS-2 expression is probably induced by hyperinsulinemia in the endothelial cells of obese subjects, the insulin-mediated Akt and eNOS activations after feeding are inadequate, and as a result, insulin-induced capillary recruitment, increase of interstitial insulin concentrations, and increase of glucose uptake by the skeletal muscle are impaired in obese subjects. Restoration of the insulin-induced eNOS phosphorylation in the endothelial cells completely reversed the reduction in the capillary recruitment and insulin delivery, and as a result, significantly restored glucose uptake by the skeletal muscle. Taken together, treatment directed at improving insulin signaling in the endothelial cells as well as myocytes may serve as a novel therapeutic strategy for ameliorating skeletal muscle insulin resistance.

Acknowledgments This work was supported by a grant for TSBMI from the Ministry of Education, Culture, Sports, Science and Technology in Japan; a Grant-in-Aid for Scientific Research in Priority Areas (A) (16209030), (A) (18209033), and (S) (20229008) from the Ministry of Education, Culture, Sports, Science, and Technology of Japan (to T. Kadowaki); and a Grant-in-Aid for Scientific Research in Priority Areas (C) (19591037) and (B) (21390279) from the Ministry of Education, Culture, Sports, Science, and Technology of Japan (to N.K.).

References

1. Chen L, Magliano DJ, Zimmet PZ. The worldwide epidemiology of type 2 diabetes mellitus present and future perspectives. Nat Rev Endocrinol. 2011;8:228–36.
2. Chan JC, Malik V, Jia W, Kadowaki T, Yajnik CS, Yoon KH, et al. Diabetes in Asia: epidemiology, risk factors, and pathophysiology. JAMA. 2009;301:2129–40.
3. Balkau B, Hu G, Qiao Q, Tuomilehto J, Borch-Johnsen K, Pyorala K. Prediction of the risk of cardiovascular mortality using a score that includes glucose as a risk factor: The DECODE Study. Diabetologia. 2004;47:2118–28.
4. Mazzone T, Chait A, Plutzky J. Cardiovascular disease risk in type 2 diabetes mellitus: insights from mechanistic studies. Lancet. 2008;371:1800–9.
5. Hogan P, Dall T, Nikolov P. American diabetes association: economic costs of diabetes in the US in 2002. Diabetes Care. 2003;26:917–32.
6. DeFronzo R, Gunnarsson R, Ojorkman O, Olsson M, Wahren J. Effects of insulin on peripheral and splanchnic glucose metabolism in noninsulin-dependent (type II) diabetes mellitus. J Clin Invest. 1985;76:149–55.
7. Turinsky J, O'Sullivan DM, Bayly BP. 1,2-Diacylglycerol and ceramide levels in insulin-resistant tissues of the rat *in vivo*. J Biol Chem. 1990;265:16880–5.
8. Dresner A, Laurent D, Marcucci M, Griffin ME, Dufour S, Cline GW, et al. Effects of free fatty acids on glucose transport and IRS-1-associated phosphatidylinositol 3-kinase activity. J Clin Invest. 1999;103:253–9.
9. Itani SI, Ruderman NB, Schmieder F, Boden G. Lipid induced insulin resistance in human muscle is associated with changes in diacylglycerol, protein kinase C, and IkappaB-alpha. Diabetes. 2002;51:2005–11.
10. Holland WL, Bikman BT, Wang LP, Yuguang G, Sargent KM, Bulchand S, et al. Lipid-induced insulin resistance mediated by the

proinflammatory receptor TLR4 requires saturated fatty acid-induced ceramide biosynthesis in mice. J Clin Invest. 2011;121:1858–70.
11. Samuel VT, Shulman GI. Mechanisms for insulin resistance: common threads and missing links. Cell. 2012;148:852–71.
12. Long YC, Zierath JR. Influence of AMP-activated protein kinase and calcineurin on metabolic networks in skeletal muscle. Am J Physiol Endocrinol Metab. 2008;295:E545–52.
13. Vincent MA, Clerk LH, Rattigan S, Clark MG, Barrett EJ. Active role for the vasculature in the delivery of insulin to skeletal muscle. Clin Exp Pharmacol Physiol. 2005;32:302–7.
14. Yang YJ, Hope ID, Ader M, Bergman RN. Insulin transport across capillaries is rate limiting for insulin action in dogs. J Clin Invest. 1989;84:1620–8.
15. Jansson PA, Fowelin JP, von Schenck HP, Smith UP, Lönnroth PN. Measurement by microdialysis of the insulin concentration in subcutaneous interstitial fluid. Importance of the endothelial barrier for insulin. Diabetes. 1993;42:1469–73.
16. Miles PD, Levisetti M, Reichart D, Khoursheed M, Moossa AR, Olefsky JM. Kinetics of insulin action *in vivo*. Identification of rate limiting steps. Diabetes. 1995;44:947–53.
17. Saltiel AR, Kahn CR. Insulin signaling and the regulation of glucose and lipid metabolism. Nature. 2001;414:799–806.
18. Nystrom FH, Quon MJ. Insulin signaling: metabolic pathways and mechanisms for specificity. Cell Signal. 1999;11:563–74.
19. Taniguchi CM, Emanuelli B, Kahn CR. Critical nodes in signaling pathways: insights into insulin action. Nat Rev Mol Cell Biol. 2006;7:85–96.
20. Boller S, Joblin BA, Xu L, Item F, Trüb T, Boschetti N, et al. From signal transduction to signal interpretation: an alternative model for the molecular function of insulin receptor substrates. Arch Physiol Biochem. 2012;118(3):148–55.
21. Abe H, Yamada N, Kamata K, Kuwaki T, Shimada M, Osuga J, et al. Hypertension, hypertriglyceridemia, and impaired endothelium-dependent vascular relaxation in mice lacking insulin receptor substrate-1. J Clin Invest. 1998;101:1784–8.
22. Kubota T, Kubota N, Moroi M, Terauchi Y, Kobayashi T, Kamata K, et al. Lack of insulin receptor substrate-2 causes progressive neointima formation in response to vessel injury. Circulation. 2003;107:3073–80.
23. Dimmeler S, Fleming I, Fisslthaler B, Hermann C, Busse R, Zeiher AM. Activation of nitric oxide synthase in endothelial cells by Akt-dependent phosphorylation. Nature. 1999;399:601–5.
24. Zeng G, Nystrom FH, Ravichandran LV, Cong LN, Kirby M, Mostowski H, et al. Roles for insulin receptor, PI3-kinase, and Akt in insulin-signaling pathways related to production of nitric oxide in human vascular endothelial cells. Circulation. 2000;101:1539–45.
25. Montagnani M, Chen H, Barr VA, Quon MJ. Insulin-stimulated activation of eNOS is independent of Ca^{2+} but requires phosphorylation byAkt at Ser(1179). J Biol Chem. 2001;276:30392–8.
26. Fleming I, Busse R. Molecular mechanisms involved in the regulation of the endothelial nitric oxide synthase. Am J Physiol Regul Integr Comp Physio. 2003;284:R1–12.
27. Rask-Madsen C, King GL. Mechanisms of disease: endothelial dysfunction in insulin resistance and diabetes. Nat Clin Pract Endocrinol Metab. 2007;3:46–56.
28. Potenza MA, Marasciulo FL, Chieppa DM, Brigiani GS, Formoso G, Quon MJ, et al. Insulin resistance in spontaneously hypertensive rats is associated with endothelial dysfunction characterized by imbalance between NO and ET-1 production. Am J Physiol. 2005;289:H813–22.
29. Potenza MA, Addabbo F, Montagnani M. Vascular actions of insulin with implications for endothelial dysfunction. Am J Physiol Endocrinol Metab. 2009;297:E568–77.
30. Kahn CR. Banting Lecture. Insulin action, diabetogenes, and the cause of type II diabetes. Diabetes. 1994;43:1066–84.
31. Ohkita M, Tawa M, Kitada K, Matsumura Y. Pathophysiological roles of endothelin receptors in cardiovascular diseases. J Pharmacol Sci. 2012;119(4):302–13.
32. Kim JA, Montagnani M, Koh KK, Quon MJ. Reciprocal relationships between insulin resistance and endothelial dysfunction: molecular and pathophysiological mechanisms. Circulation. 2006;113:1888–904.
33. Calles-Escandon J, Cipolla M. Diabetes and endothelial dysfunction: a clinical perspective. Endocr Rev. 2001;22:36–52.
34. Jansson PA. Endothelial dysfunction in insulin resistance and type 2 diabetes. J Intern Med. 2007;262:173–83.
35. Naruse K, Rask-Madsen C, Takahara N, Ha SW, Suzuma K, Way KJ, et al. Activation of vascular protein kinase C-beta inhibits Akt-dependent endothelial nitric oxide synthase function in obesity-associated insulin resistance. Diabetes. 2006;55:691–8.
36. Jiang ZY, Lin YW, Clemont A, Feener EP, Hein KD, Igarashi M, et al. Characterization of selective resistance to insulin signaling in the vasculature ofobese Zucker (fa/fa) rats. J Clin Invest. 1999;104:447–57.
37. Gogg S, Smith U, Jansson PA. Increased MAPK activation and impaired insulin signaling in subcutaneous microvascular endothelial cells in type 2 diabetes: the role of endothelin-1. Diabetes. 2009;58:2238–45.
38. Kubota T, Kubota N, Kumagai H, Yamaguchi S, Kozono H, Takahashi T, et al. Impaired insulin signaling in endothelial cells reduces insulin-induced glucose uptake by skeletal muscle. Cell Metab. 2011;13:294–307.
39. Zhang J, Ou J, Bashmakov Y, Horton JD, Brown MS, Goldstein JL. Insulin inhibits transcription of IRS-2 gene in rat liver through an insulin response element (IRE) that resembles IREs of other insulin-repressed genes. Proc Natl Acad Sci USA. 2001;98:3756–61.
40. Ide T, Shimano H, Yahagi N, Matsuzaka T, Nakakuki M, Yamamoto T, et al. SREBPs suppress IRS-2-mediated insulin signaling in the liver. Nat Cell Biol. 2004;6:351–7.
41. Sherwin RS, Kramer KJ, Tobin JD, Insel PA, Liljenquist JE, Berman M, et al. A model of the kinetics of insulin in man. J Clin Invest. 1974;53:1481–92.
42. DeFronzo RA, Tobin JD, Andres R. Glucose clamp technique: a method for quantifying insulin secretion and resistance. Am J Physiol. 1979;237:E214–23.
43. Chiu JD, Richey JM, Harrison LN, Zuniga E, Kolka CM, Kirkman E, et al. Direct administration of insulin into skeletal muscle reveals that the transport of insulin across the capillary endothelium limits the time course of insulin to activate glucose disposal. Diabetes. 2008;57:828–35.
44. Prager R, Wallace P, Olefsky JM. *In vivo* kinetics of insulin action on peripheral glucose disposal and hepatic glucose output in normal and obese subjects. J Clin Invest. 1986;78:472–81.
45. Turk D, Alzaid A, Dinneen S, Nair KS, Rizza R. The effects of non-insulin-dependent diabetes mellitus on the kinetics of onset of insulin action in hepatic and extrahepatic tissues. J Clin Invest. 1995;95:755–62.
46. Sjöstrand M, Gudbjörnsdottir S, Holmäng A, Lönn L, Strindberg L, Lönnroth P. Delayed transcapillary transport of insulin to muscle interstitial fluid in obese subjects. Diabetes. 2002;51:2742–8.
47. Aird WC. Phenotypic heterogeneity of the endothelium: I. Structure, function, and mechanisms. Circ Res. 2007;100:158–73.
48. King GL, Johnson SM. Receptor-mediated transport of insulin across endothelial cells. Science. 1985;227:1583–6.
49. Demovsek KD, Bar RS. Processing of cell-bound insulin by capillary and macrovascular endothelial cells in culture. Am J Physiol. 1985;248:E244–51.
50. Schnitzer JE, Oh P, Pinney E, Allard J. Filipin-sensitive caveolae-mediated transport in endothelium: reduced transcytosis, scavenger endocytosis, and capillary permeability of select macromolecules. J Cell Biol. 1994;127:1217–32.

51. Steil GM, Ader M, Moore DM, Rebrin K, Bergman RN. Transendothelial insulin transport is not saturable *in vivo*. No evidence for a receptor-mediated process. J Clin Invest. 1996;97:1497–503.
52. Hamilton-Wessler M, Ader M, Dea MK, Moore D, Loftager M, Markussen J, et al. Mode of transcapillary transport of insulin and insulin analog NN304in dog hindlimb: evidence for passive diffusion. Diabetes. 2002;51:574–82.
53. Majumdar S, Genders AJ, Inyard AC, Frison V, Barrett EJ. Insulin entry into muscle involves a saturable process in the vascular endothelium. Diabetologia. 2012;55:450–6.
54. Barrett EJ, Wang H, Upchurch CT, Liu Z. Insulin regulates its own delivery to skeletal muscle by feed-forward actions on the vasculature. Am J Physiol Endocrinol Metab. 2011;30:E252–63.
55. Wang H, Liu Z, Li G, Barrett EJ. The vascular endothelial cell mediates insulin transport into skeletal muscle. Am J Physiol Endocrinol Metab. 2006;291:E323–32.
56. Wang H, Wang AX, Barrett EJ. Caveolin-1 is required for vascular endothelial insulin uptake. Am J Physiol Endocrinol Metab. 2011;300:E134–44.
57. Schubert W, Frank PG, Woodman SE, Hyogo H, Cohen DE, Chow CW, et al. Microvascular hyperpermeability in caveolin-1 (−/−) knock-out mice. Treatment with a specific nitric-oxide synthase inhibitor, L-NAME, restores normal microvascular permeability in Cav-1 null mice. J Biol Chem. 2002;277:40091–8.
58. Rattigan S, Clark MG, Barrett EJ. Hemodynamic actions of insulin in rat skeletal muscle: evidence for capillary recruitment. Diabetes. 1997;46:1381–8.
59. Parks DA, Granger DN. Xanthine oxidase: biochemistry, distribution and physiology. Acta Physiol Scand Suppl. 1986;548:87–99.
60. Wei K, Jayaweera AR, Firoozan S, Linka A, Skyba DM, Kaul S. Quantification of myocardial blood flow with ultrasound-induced destruction of microbubbles administered as a constant venous infusion. Circulation. 1998;97:473–83.
61. Clark MG. Impaired microvascular perfusion: a consequence of vascular dysfunction and a potential cause of insulin resistance in muscle. Am J Physiol Endocrinol Metab. 2008;295:E732–50.
62. Barrett EJ, Eggleston EM, Inyard AC, Wang H, Li G, Chai W, et al. The vascular actions of insulin control its delivery to muscle and regulate the rate-limiting step in skeletal muscle insulin action. Diabetologia. 2009;52:752–64.
63. Vincent MA, Dawson D, Clark AD, Lindner JR, Rattigan S, Clark MG, et al. Skeletal muscle microvascular recruitment by physiological hyperinsulinemia precedes increases in total blood flow. Diabetes. 2002;51:42–8.
64. Duplain H, Burcelin R, Sartori C, Cook S, Egli M, Lepori M, et al. Insulin resistance, hyperlipidemia, and hypertension in mice lacking endothelial nitric oxide synthase. Circulation. 2001;104:342–5.
65. Vincent MA, Barrett EJ, Lindner JR, Clark MG, Rattigan S. Inhibiting NOS blocks microvascular recruitment and blunts glucose uptake in response to insulin. Am J Physiol Endocrinol Metab. 2003;285:E123–9.
66. Scherrer U, Randin D, Vollenweider P, Vollenweider L, Nicod P. Nitric oxide release accounts for insulin's vascular effects in humans. J Clin Invest. 1994;94:2511–5.
67. Andreozzi F, Laratta E, Procopio C, Hribal ML, Sciacqua A, Perticone M, et al. Interleukin-6 impairs the insulin signaling pathway, promoting production of nitric oxide in human umbilical vein endothelial cells. Mol Cell Biol. 2007;27:2372–83.
68. Federici M, Pandolfi A, De Filippis EA, Pellegrini G, Menghini R, Lauro D, et al. G972R1RS-1 variant impairs insulin regulation of endothelial nitric oxide synthase in cultured human endothelial cells. Circulation. 2004;109:399–405.
69. Kainoh M, Maruyama I, Nishio S, Nakadate T. Enhancement by beraprost sodium, a stable analogue of prostacyclin, in thrombomodulin expression on membrane surface of cultured vascular endothelial cells via increase in cyclic AMP level. Biochem Pharmacol. 1991;41:1135–40.
70. Niwano K, Arai M, Tomaru K, Uchiyama T, Ohyama Y, Kurabayashi M. Transcriptional stimulation of the eNOS gene by the stable prostacyclin analogue beraprost is mediated through cAMP-responsive element in vascular endothelial cells: close link between PGI2 signal and NO pathways. Circ Res. 2003;93:523–30.
71. Lièvre M, Morand S, Besse B, Fiessinger J, Boissel J. Oral Beraprost sodium, a prostaglandin I2 analogue, for intermittent claudication: a double-blind, randomized, multicenter controlled trial. Beraprostet Claudication Intermittente (BERCI) Research Group. Circulation. 2000;102:426–31.
72. Galiè N, Humbert M, Vachiéry JL, Vizza CD, Kneussl M, Manes A, et al. Arterial Pulmonary Hypertension and Beraprost European (ALPHABET) study group effects of beraprost sodium, an oral prostacyclin analogue, in patients with pulmonary arterial hypertension: a randomized, double-blind, placebo-controlled trial. J Am Coll Cardiol. 2002;39:1496–502.
73. Lovshin JA, Drucker DJ. Incretin-based therapies for type 2 diabetes mellitus. Nat Rev Endocrinol. 2009;5:262–9.
74. Richter G, Feddersen O, Wagner U, Barth P, Göke R, Göke B. GLP-1 stimulates secretion of macromolecules from airways and relaxes pulmonary artery. Am J Physiol. 1993;265:L374–81.
75. Nyström T, Gutniak MK, Zhang Q, Zhang F, Holst JJ, Ahrén B, et al. Effects of glucagon-like peptide-1 on endothelial function in type 2 diabetes patients with stable coronary artery disease. Am J Physiol Endocrinol Metab. 2004;287:E1209–15.
76. Erdogdu O, Nathanson D, Sjöholm A, Nyström T, Zhang Q. Exendin-4 stimulates proliferation of human coronary artery endothelial cells through eNOS-, PKA- and PI3K/Akt-dependent pathways and requires GLP-1 receptor. Mol Cell Endocrinol. 2010;325:26–35.
77. Chai W, Dong Z, Wang N, Wang W, Tao L, Cao W, et al. Glucagon-like peptide 1 recruits microvasculature and increases glucose use in muscle via a nitric oxide-dependent mechanism. Diabetes. 2012;61:888–96.
78. Clerk LH, Rattigan S, Clark MG. Lipid infusion impairs physiologic insulin-mediated capillary recruitment and muscle glucose uptake *in vivo*. Diabetes. 2002;51:1138–45.
79. Youd JM, Rattigan S, Clark MG. Acute impairment of insulin-mediated capillary recruitment and glucose uptake in rat skeletal muscle *in vivo* by TNF-alpha. Diabetes. 2000;49:1904–9.
80. Zhang L, Wheatley CM, Richards SM, Barrett EJ, Clark MG, Rattigan S. TNF-alpha acutely inhibits vascular effects of physiological but not high insulin or contraction. Am J Physiol Endocrinol Metab. 2003;285:E654–60.
81. Wallis MG, Smith ME, Kolka CM, Zhang L, Richards SM, Rattigan S, et al. Acute glucosamine-induced insulin resistance in muscle *in vivo* is associated with impaired capillary recruitment. Diabetologia. 2005;48:2131–9.
82. Wallis MG, Wheatley CM, Rattigan S, Barrett EJ, Clark AD, Clark MG. Insulin-mediated hemodynamic changes are impaired in muscle of zucker obese rats. Diabetes. 2002;51:3492–8.
83. Jaap AJ, Hammersley MS, Shore AC, Tooke JE. Reduced microvascular hyperaemia in subjects at risk of developing type 2(non-insulin-dependent) diabetes mellitus. Diabetologia. 1994;37:214–6.
84. Caballero AE, Arora S, Saouaf R, Lim SC, Smakowski P, Park JY, et al. Microvascular and macrovascular reactivity is reduced in subjects at risk for type 2diabetes. Diabetes. 1999;48:1856–62.
85. Serné EH, de Jongh RT, Eringa EC, Ijzerman RG, de Boer MP, Stehouwer CD. Microvascular dysfunction: causative role in the association between hypertension, insulin resistance and the metabolic syndrome. Essays Biochem. 2006;42:163–76.